JHEP

Published for SISSA by Springer

Received: May 10, 2017
Accepted: June 5, 2017
Published: June 20, 2017

Superparticle phenomenology from the natural mini-landscape

Howard Baer,[a] **Vernon Barger,**[b] **Michael Savoy,**[a] **Hasan Serce**[a] **and Xerxes Tata**[c]

[a] *Department of Physics and Astronomy, University of Oklahoma, Norman, OK 73019, U.S.A.*

[b] *Department of Physics, University of Wisconsin, Madison, WI 53706, U.S.A.*

[c] *Department of Physics and Astronomy, University of Hawaii, Honolulu, HI 96822, U.S.A.*

E-mail: baer@nhn.ou.edu, barger@pheno.wisc.edu, savoy@ou.edu, serce@ou.edu, tata@phys.hawaii.edu

Abstract: The methodology of the heterotic *mini-landscape* attempts to zero in on phenomenologically viable corners of the string landscape where the effective low energy theory is the Minimal Supersymmetric Standard Model with localized grand unification. The gaugino mass pattern is that of mirage-mediation. The magnitudes of various SM Yukawa couplings point to a picture where scalar soft SUSY breaking terms are related to the geography of fields in the compactified dimensions. Higgs fields and third generation scalars extend to the bulk and occur in split multiplets with TeV scale soft masses. First and second generation scalars, localized at orbifold fixed points or tori with enhanced symmetry, occur in complete GUT multiplets and have much larger masses. This picture can be matched onto the parameter space of generalized mirage mediation. Naturalness considerations, the requirement of the observed electroweak symmetry breaking pattern, and LHC bounds on $m_{\tilde{g}}$ together limit the gravitino mass to the $m_{3/2} \sim 5$–60 TeV range. The mirage unification scale is bounded from below with the limit depending on the ratio of squark to gravitino masses. We show that while natural SUSY in this realization may escape detection even at the high luminosity LHC, the high energy LHC with $\sqrt{s} = 33$ TeV could unequivocally confirm or exclude this scenario. It should be possible to detect the expected light higgsinos at the ILC if these are kinematically accessible, and possibly also discriminate the expected compression of gaugino masses in the natural mini-landscape picture from the mass pattern expected in models with gaugino mass unification. The thermal WIMP signal should be accessible via direct detection searches at the multi-ton noble liquid detectors such as XENONnT or LZ.

Keywords: Supersymmetry Phenomenology

ArXiv ePrint: 1705.01578

https://doi.org/10.1007/JHEP06(2017)101

JHEP06(2017)101

Contents

1 Introduction **1**

2 Natural generalized mirage mediation **4**

3 Superparticle spectra from the natural mini-landscape **6**
3.1 A natural mini-landscape benchmark point 6

4 Scan over natural mini-landscape parameter space **13**
4.1 Results for $m_0(1,2) \simeq m_{3/2}$ 13
4.1.1 The mini2 benchmark model 14
4.2 Effect of relaxing $m_0(1,2) \simeq m_{3/2}$ 17

5 Implications for LHC, ILC and dark matter searches **18**
5.1 Consequences for LHC and LHC33 18
5.2 Consequences for ILC 22
5.3 Consequences for WIMP and axion searches 23

6 Conclusions **25**

JHEP06(2017)101

1 Introduction

String theory offers a UV complete finite theory which includes a quantum mechanical treatment of gravity and the possible inclusion of the Standard Model (SM) [1, 2]. While only a few string theories exist, formulated as 10-dimensional superstring or 11-dimensional M-theory, the compactification of the extra-dimensions leads to a vast landscape for 4-D theories. It appears that neither the SM nor its minimal supersymmetric extension are a *generic* part of the landscape. There has, nevertheless, been a vast effort to understand how either of these models might emerge from the landscape of string vacua [3].

One promising approach has been to adopt the SM as a low energy target effective field theory and to see if it might arise in special regions of the string landscape. By investigating these so-called "fertile patches" of the landscape, lessons may be learned about how the SM might emerge from string theory compactification [4]. Since string theory necessarily involves a high mass scale $M_{\rm string}$ close to $m_{\rm Pl}$ or $m_{\rm GUT}$, low energy ($N = 1$) supersymmetry (SUSY) is usually invoked to stabilize the Higgs mass [5–7], and the low energy target effective theory is frequently taken as the Minimal Supersymetric Standard Model (MSSM). The MSSM enjoys indirect phenomenological support in that 1. the measured values of weak scale gauge couplings unify under MSSM renormalization group running at $Q = m_{\rm GUT} \simeq 2 \times 10^{16}$ GeV [8–11], 2. the measured value of m_t is just what is needed to drive a radiative breakdown of electroweak symmetry [12–20], and 3. the

measured value of the Higgs boson mass $m_h \simeq 125\,\text{GeV}$ [21, 22] falls squarely within the required MSSM range where $m_h \lesssim 135\,\text{GeV}$ is required [23–26].[1]

A very practical avenue for linking string theory to weak scale physics, known as the mini-landscape, has been investigated at some length [30, 31]. The methodology of the mini-landscape is to zero in on the small subset of landscape vacua which give rise to reasonable weak scale particle physics as realized by the MSSM. The mini-landscape adopts the $E_8 \times E_8$ gauge structure of the heterotic string since one of the E_8 groups automatically contains as sub-groups the grand unified structures that the SM multiplets and quantum numbers seems to reflect: $E_8 \supset E_6 \supset \text{SO}(10) \supset \text{SU}(5) \supset G_{\text{SM}}$ where $G_{\text{SM}} \equiv \text{SU}(3)_C \times \text{SU}(2)_L \times \text{U}(1)_Y$. The other E_8 may contain a hidden sector with SU(n) subgroups which become strongly interacting at some intermediate scale $\Lambda \sim 10^{13}\,\text{GeV}$ leading to gaugino condensation and consequent supergravity breaking [32–35]. Compactification of the heterotic string on a $Z_6 - II$ orbifold [36] can lead to low energy theories which include the MSSM, possibly with additional exotic matter states.

A detailed exploration of the mini-landscape has been performed a number of years ago. In this picture, the properties of the 4-D low energy theory are essentially determined by the geometry of the compact manifold, and by the location of the matter superfields on this manifold. The gauge group is G_{SM} though the symmetry may be enhanced for fields confined to fixed points, or to fixed tori, in the extra dimensions. Examination of the models which lead to MSSM-like structures revealed the following picture [37].

1. The first two generations of matter live on orbifold fixed points which exhibit the larger SO(10) gauge symmetry; thus, first and second generation fermions fill out the 16-dimensional spinor representation of SO(10).

2. The Higgs multiplets H_u and H_d live in the untwisted sector and are bulk fields that feel just G_{SM}. As such, they (and the gauge bosons) come in incomplete GUT multiplets which automatically solves the classic doublet-triplet splitting problem.

3. The third generation quark doublet and the top singlet also reside in the bulk, and thus have large overlap with the Higgs fields and correspondingly large Yukawa couplings. The location of other third generation matter fields is model dependent. The small overlap of Higgs and first/second generation fields (which do not extend into the bulk) accounts for their much smaller Yukawa couplings.

4. Supergravity breaking may arise from hidden sector gaugino condensation with $m_{3/2} \sim \Lambda^3/m_{\text{Pl}}^2$ with the gaugino condensation scale $\Lambda \sim 10^{13}\,\text{GeV}$. SUSY breaking effects are felt differently by the various MSSM fields as these are located at different places in the compact manifold. Specifically, the Higgs and top squark fields in the untwisted sector feel extended supersymmetry (at tree level) in 4-dimensions, and are thus more protected than the fields on orbifold fixed points which receive protection from just $N = 1$ supersymmetry [38, 39]. First/second generation matter scalars are thus expected with masses $\sim m_{3/2}$. Third generation and Higgs soft mass

[1] For some related approaches, see [27–29].

JHEP06(2017)101

parameters (which enjoy the added protection from extended SUSY) are suppressed by an additional loop factor $\sim 4\pi^2 \sim \log(m_{\rm Pl}/m_{3/2})$. Gaugino masses and trilinear soft terms are expected to be suppressed by the same factor. The suppression of various soft SUSY breaking terms means that (anomaly-mediated) loop contributions [40–43] may be comparable to modulus- (gravity-) mediated contributions leading to models with mixed moduli-anomaly mediation [44–48] (usually dubbed as *mirage mediation* or MM for short); in these scenarios, gaugino masses apparently unify at some intermediate scale

$$\mu_{\rm mir} \sim m_{\rm GUT} e^{-8\pi^2/\alpha}, \tag{1.1}$$

where α parametrizes the relative amounts of moduli- versus anomaly-mediation.

The phenomenon of mirage mediation was originally found to occur in type-IIB strings where moduli fields were stabilized by a combination of fluxes and gaugino condensation leading to theories with an AdS vacuum. Uplifting of the AdS to a de Sitter vacuum was arranged via the presence of anti-$D3$ branes (KKLT formulation [49]). Since these original models were first written down, additional uplifting mechanisms have been formulated [50–57]. The mirage mediation SUSY breaking scheme was also found to arise in compactification of the heterotic string in addition to the original II-B proposal [58].

The mirage mediation soft SUSY breaking Lagrangian terms have been computed in a number of papers and are given by [44–48, 59, 60],

$$M_a = M_s(\alpha + b_a g_a^2)\,, \tag{1.2}$$
$$A_{ijk} = M_s(-a_{ijk}\alpha + \gamma_i + \gamma_j + \gamma_k)\,, \tag{1.3}$$
$$m_i^2 = M_s^2(c_i\alpha^2 + 4\alpha\xi_i - \dot\gamma_i)\,, \tag{1.4}$$

where $M_s \equiv \frac{m_{3/2}}{16\pi^2}$, b_a are the gauge β function coefficients for gauge group a and g_a are the corresponding gauge couplings. The coefficients that appear in (1.2)–(1.4) are given by $c_i = 1 - n_i$, $a_{ijk} = 3 - n_i - n_j - n_k$ and $\xi_i = \sum_{j,k} a_{ijk}\frac{y_{ijk}^2}{4} - \sum_a g_a^2 C_2^a(f_i)$. Finally, y_{ijk} are the superpotential Yukawa couplings, C_2^a is the quadratic Casimir for the a$^{\rm th}$ gauge group corresponding to the representation to which the sfermion $\tilde f_i$ belongs, γ_i is the anomalous dimension, and $\dot\gamma_i = 8\pi^2\frac{\partial\gamma_i}{\partial\log\mu}$. Expressions for the last two quantities involving the anomalous dimensions can be found in the appendix of ref. [60, 61].

In the earliest models the coefficients that appear in (1.3) and (1.4) took on values determined by discrete values of the modular weights n_i which depended on the location of fields in the original II-B string model and were given by $c_i = 1 - n_i$, $a_{ijk} = 3 - n_i - n_j - n_k$. Thus, the parameter space of the original MM models was given by

$$m_{3/2}\,,\ \alpha\,,\ \tan\beta\,,\ {\rm sign}(\mu)\,,\ n_i\,. \tag{1.5}$$

It has since been recognized that while the gaugino mass patterns in eq. (1.2) are a robust prediction of the mirage-mediation picture, the corresponding patterns of scalar mass and trilinear parameters are sensitive to the mechanisms of moduli stabilization and uplifting. This, together with the fact that the original mirage-mediation models seemed

JHEP06(2017)101

to require relatively large fine-tuning in light of the measured value of the Higgs boson mass [64], led us to suggest a phenomenological generalization of this picture discussed in section 2 [65]. This extension allows us to accommodate the mass patterns suggested by the mini-landscape picture mentioned above, the phenomenology of which is the subject of this paper. In section 3 we explore the parameter space of this generalized mirage mediation (GMM) framework, identify portions which are consistent with naturalness, and study the resulting sparticle spectra expected in the natural mini-landscape picture. In section 4, we perform scans over parameter space to obtain upper bounds on superpartner masses from naturalness requirements. Section 5, we broadly discuss collider and dark matter phenomenology of the natural mini-landscape picture. We summarize our main results in section 6.

2 Natural generalized mirage mediation

We have just mentioned that the original MM models based on the parameter space (1.5) were found to be highly fine-tuned even under the most conservative electroweak fine-tuning measure $\Delta_{\rm EW}$ [62, 63] for parameter choices which gave rise to $m_h \sim 123$–$127\,{\rm GeV}$ [64]. The electroweak fine-tuning measure $\Delta_{\rm EW}$ is defined by requiring that there are no large cancellations between independent contributions to the Z boson mass calculated from the minimization conditions of the 1-loop MSSM scalar potential,

$$\frac{m_Z^2}{2} = \frac{m_{H_d}^2 + \Sigma_d^d - (m_{H_u}^2 + \Sigma_u^u)\tan^2\beta}{\tan^2\beta - 1} - \mu^2. \tag{2.1}$$

Here Σ_u^u and Σ_d^d denote 1-loop corrections (expressions can be found in the appendix of ref. [63]) to the scalar potential, $m_{H_u}^2$ and $m_{H_d}^2$ are the weak scale values of the soft breaking Higgs masses and $\tan\beta \equiv \langle H_u\rangle/\langle H_d\rangle$. SUSY models requiring large cancellations between the various terms on the right-hand-side of eq. (2.1) to reproduce the measured value of m_Z^2 are regarded as unnatural, or fine-tuned. Thus, natural SUSY models are characterized by low values of the *electroweak* naturalness measure $\Delta_{\rm EW}$ defined as [62, 63]

$$\Delta_{\rm EW} \equiv \max|\text{each term on r.h.s. of eq. (2.1)}|/(m_Z^2/2)\,. \tag{2.2}$$

It is essential that the sensitivity of m_Z be evaluated only with respect to the *independent* parameters of the theory. If this is not done, the UV sensitivity of the theory will be over-estimated, and the theory may be incorrectly regarded as fine-tuned. It has further been shown that traditionally used high scale measures of fine-tuning [66–68] reduce to $\Delta_{\rm EW}$ once underlying (potential) correlations between parameters are properly incorporated [64, 69, 70]. For this reason, we regard $\Delta_{\rm EW}$ as the most conservative measure of fine-tuning.

It seems highly implausible that if the SUSY breaking parameter $m_{H_u}^2$ runs large negative such that $-m_{H_u}^2 \gg m_Z^2$, then the value of the SUSY-conserving parameter μ, which likely has a very different origin from the soft terms, would be of just the right value to nearly cancel against $-m_{H_u}^2$ and yield the (much smaller) observed value of m_Z. *Electroweak naturalness* then implies that

JHEP06(2017)101

- $m_{H_u}^2 \sim -(100\text{–}300)^2\,\mathrm{GeV}^2$, and
- $\mu^2 \sim (100\text{–}300)^2\,\mathrm{GeV}^2$ [71, 72]

(the closer to m_Z the better). For moderate-to-large $\tan\beta \gtrsim 5$, the remaining contributions other than Σ_u^u are suppressed. The largest radiative corrections Σ_u^u typically come from the top squark sector. The value of the trilinear soft term $A_0 \sim -1.6m_0$ leads to TeV-scale top squarks and minimizes $\Sigma_u^u(\tilde{t}_{1,2})$ while simultaneously lifting the Higgs mass m_h to $\sim 125\,\mathrm{GeV}$ [63].

The failure of naturalness in MM as detailed above has led us previously to propose moving from discrete choices of the parameters a_{ijk} and c_i in eqs. (1.3) and (1.4) to a continuous range, and also to allow c_i values greater than 1 [65]. While the discrete parameter choices occur in a wide range of KKLT-type compactifications (for some discussion, see ref. [73]), a continuous range of these parameters may be expected if one allows for more general methods of moduli stabilization and potential uplifting. For instance, if the soft terms scan as in the string landscape picture [74], then their moduli-mediated contributions may be expected to be parametrized by a continuous value. For models which generate a small μ term $\sim 100\,\mathrm{GeV}$ from multi-TeV soft terms, such as in the Kim-Nilles mechanism [75] with radiative Peccei-Quinn breaking [76], it has been suggested that the statistical pull by the landscape towards large soft terms, coupled with the anthropic requirement of $m_{\mathrm{weak}} \sim 100\,\mathrm{GeV}$, acts as an attractor towards natural SUSY soft term boundary conditions [77].

Note that the phenomenological modification we have suggested will not affect the result eq. (1.2) for gaugino mass parameters, which has been stressed [78] to be the most robust prediction of the MM mechanism. In this paper, we allow for the more *general* mirage mediation (GMM) parameters, thus adopting a parameter space given by

$$\alpha\,,\ m_{3/2}\,,\ c_m\,,\ c_{m3}\,,\ a_3\,,\ c_{H_u}\,,\ c_{H_d}\,,\ \tan\beta \quad (\mathrm{GMM})\,, \tag{2.3}$$

where a_3 is short for $a_{Q_3H_uU_3}$. Here, we adopt an independent value c_m for the first two matter-scalar generations whilst the parameter c_{m3} applies to third generation matter scalars. This splitting accomodates the case of the mini-landscape wherein third generation scalars are expected to receive soft terms $\sim$TeV whilst first/second generation matter scalars are expected to occur with mass values $\sim m_{3/2} \gg 1\,\mathrm{TeV}$. The independent values of c_{H_u} and c_{H_d} which set the moduli-mediated contribution to the soft Higgs mass terms may conveniently be traded for weak scale values of μ and m_A as is done in the two-parameter non-universal Higgs model (NUHM2) [79–83]:

$$\alpha\,,\ m_{3/2}\,,\ c_m\,,\ c_{m3}\,,\ a_3\,,\ \tan\beta\,,\ \mu\,,\ m_A \quad (\mathrm{GMM}')\,. \tag{2.4}$$

This procedure allows for more direct exploration of natural SUSY parameter space which requires $\mu \sim 100\text{–}300\,\mathrm{GeV}$ (the closer to m_Z the better). Thus, our final relevant soft terms

JHEP06(2017)101

are given by

$$M_a = (\alpha + b_a g_a^2) m_{3/2}/16\pi^2, \tag{2.5}$$
$$A_\tau = (-a_3\alpha + \gamma_{L_3} + \gamma_{H_d} + \gamma_{E_3}) m_{3/2}/16\pi^2, \tag{2.6}$$
$$A_b = (-a_3\alpha + \gamma_{Q_3} + \gamma_{H_d} + \gamma_{D_3}) m_{3/2}/16\pi^2, \tag{2.7}$$
$$A_t = (-a_3\alpha + \gamma_{Q_3} + \gamma_{H_u} + \gamma_{U_3}) m_{3/2}/16\pi^2, \tag{2.8}$$
$$m_i^2(1,2) = (c_m\alpha^2 + 4\alpha\xi_i - \dot{\gamma}_i)(m_{3/2}/16\pi^2)^2, \tag{2.9}$$
$$m_j^2(3) = (c_{m3}\alpha^2 + 4\alpha\xi_j - \dot{\gamma}_j)(m_{3/2}/16\pi^2)^2, \tag{2.10}$$
$$m_{H_u}^2 = (c_{H_u}\alpha^2 + 4\alpha\xi_{H_u} - \dot{\gamma}_{H_u})(m_{3/2}/16\pi^2)^2, \tag{2.11}$$
$$m_{H_d}^2 = (c_{H_d}\alpha^2 + 4\alpha\xi_{H_d} - \dot{\gamma}_{H_d})(m_{3/2}/16\pi^2)^2, \tag{2.12}$$

where, for a given value of α and $m_{3/2}$, the values of c_{H_u} and c_{H_d} are adjusted so as to fulfill the input values of μ and m_A. In the above expressions, the index i runs over first/second generation MSSM scalars $i = Q_{1,2}, U_{1,2}, D_{1,2}, L_{1,2}$ and $E_{1,2}$ while j runs overs third generation scalars $j = Q_3, U_3, D_3, L_3$ and E_3. The common value of c_m in eq. (2.9) ensures that flavor-changing neutral current (FCNC) processes are suppressed. The GMM parameter space is well-suited for the exploration of the superparticle mass spectra and resulting phenomenology that is to be expected from the natural mini-landscape. With this in mind, we have recently included the GMM model as model line #12 into the event generator program Isajet 7.86 [84, 85].

3 Superparticle spectra from the natural mini-landscape

We begin by reminding the reader that in the natural mini-landscape picture, 1. the gaugino mass spectrum is as given by mirage mediation eq. (2.5), 2. $|\mu|$ not far from m_Z, 3. third generation squarks lie in the TeV range, and 4. first and second generation masses are close to $m_{3/2} \sim$ multi-TeV. To obtain a broad overview, we show in figure 1 the value of M_3(weak) (where $m_{\tilde{g}} \sim M_3$(weak) up to loop corrections) as generated using eq. (2.5) — but scaled by a factor $M_3(\text{weak}) \simeq 2.34 M_3(\text{GUT})$ to account roughly for RG evolution — without making a specific assumption about scalar sector parameters. From the figure, we immediately see that the LHC13 limit $m_{\tilde{g}} \lesssim 1.9\,\text{TeV}$ [86, 87], roughly speaking, excludes values of α below the $M_3(\text{weak}) = 1.9\,\text{TeV}$ contour. Moreover, the fact that the naturalness condition bounds the gluino mass from above similarly excludes values of α above the dashed curve if one insists on EW naturalness with $\Delta_{\text{EW}} < 30$ [88]. We regard the large range of $m_{3/2}$ and α between these curves as the "favoured region" of the mini-landscape picture, but keep in mind that the boundaries have some fuzziness in part because the curves are only approximate contours of the gluino mass. We will see later that — for natural sparticle mass spectra from the mini-landscape — $m_{3/2}$ is in fact bounded from above, the exact bound depending on the details of the mini-landscape picture.

3.1 A natural mini-landscape benchmark point

To gain some perspective on natural mini-landscape parameter space, we first generate a benchmark (BM) point using Isajet 7.86. We adopt a value $m_{3/2} = 10\,\text{TeV}$ and then

JHEP06(2017)101

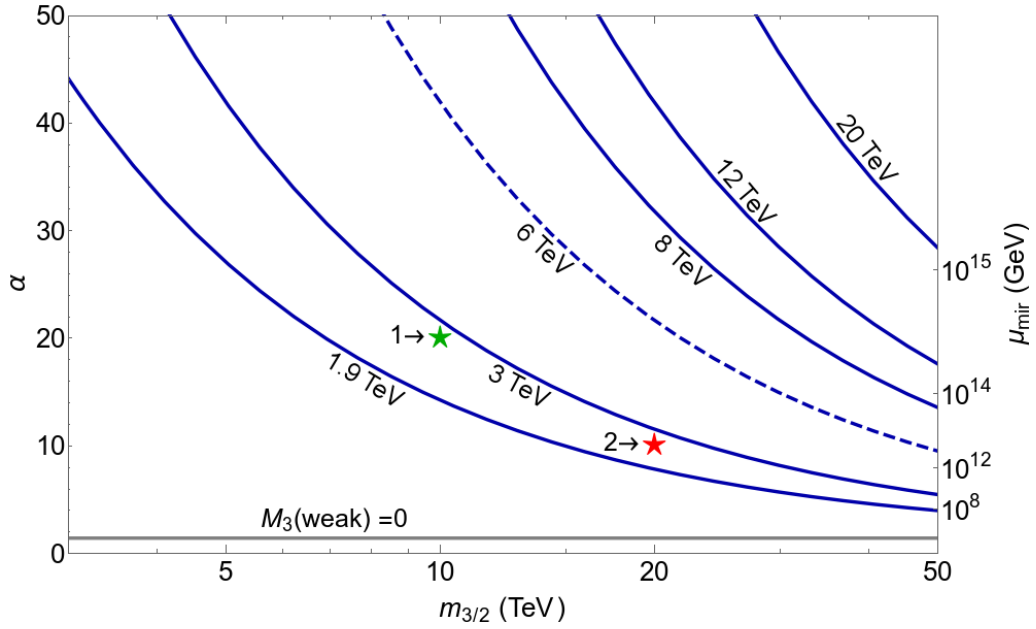

Figure 1. Contours of M_3(weak) in the α vs. $m_{3/2}$ plane of the GMM model. The region below $M_3 \sim 1.9$ is excluded by LHC gluino pair searches. The locations of the benchmark points mini1 and mini2 are shown by green and red stars, respectively. The region below the dashed $M_3 \sim 6\,\text{TeV}$ contour has the capacity to be natural. On the right side, some corresponding values of $\mu_{\rm mir}$ are shown.

select a value of $\alpha = 20$ well within the allowed region of figure 1, the location of which is shown by the green star. To obtain the first two generation mass parameters $\sim m_{3/2}$ we choose $c_m = 100$ in eq. (2.9). This leads to first/second generation soft terms $\sim 12.7\,\text{TeV}$. To gain third generation scalars in the several TeV range, we select $c_{m3} = 18$ leading to $m_i(3) \sim 5.4\,\text{TeV}$. A choice of $a_3 \sim 6$ leads to a GUT scale trilinear soft term $A_t \sim -7.6\,\text{TeV}$ which is a typical value required to boost the Higgs mass m_h up to its measured value $\sim 125\,\text{GeV}$ [89] whilst simultaneously reducing $\Delta_{\rm EW}$ to natural values [62]. In addition, we choose a natural value of $\mu = 150\,\text{GeV}$, with $\tan\beta = 10$ and $m_A = 2\,\text{TeV}$. The sparticle spectrum from Isajet 7.86 is listed in table 1 as the BM point mini1. The spectrum for an NUHM3 model that should be in close correspondence with the BM mini1 point is shown in the adjacent column of this table.[2] The last column lists the spectrum and parameters of a second mini-landscape point introduced in section 4.1.1. From the table, we see that for the mini1 BM point the first/second generation matter scalars lie at $m_i(1,2) \sim 12.8\,\text{TeV}$ while third generation scalars are in the several TeV range with $m_{\tilde{t}_1} = 1564\,\text{GeV}$. The gluino comes in at 2.9 TeV. Both $m_{\tilde{g}}$ and $m_{\tilde{t}_1}$ are well above current LHC13 limits. The

[2]The NUHM3 model is a three parameter extension of the familiar mSUGRA/CMSSM model in which the two GUT scale Higgs mass parameters as well as the GUT scale third generation sfermion mass parameters are taken to be independent of the universal scalar mass m_0 of the mSUGRA framework. The mini-landscape picture is then very close to the NUHM3 picture except that the GUT scale gaugino mass pattern is given by mirage mediation, and that scalar masses and A-parameters include small anomaly-mediated contributions.

JHEP06(2017)101

parameter	mini1	NUHM3	mini2
$m_{3/2}$	10000	–	20000
α	20	–	10
c_m	100	–	250
c_{m3}	18	–	23
a_3	6	–	6
$\tan\beta$	10	10	10
μ	150	150	150
m_A	2000	2000	2000
$m_{\tilde{g}}$	2911.5	2916.2	2784.5
$m_{\tilde{u}_L}$	12810.5	12754.5	20097.5
$m_{\tilde{u}_R}$	12888.2	12830.6	20177.8
$m_{\tilde{e}_R}$	12589.0	12525.1	19965.9
$m_{\tilde{t}_1}$	1564.5	1787.2	1341.7
$m_{\tilde{t}_2}$	3805.3	3869.5	3671.2
$m_{\tilde{b}_1}$	3840.5	3899.5	3709.6
$m_{\tilde{b}_2}$	5306.0	5321.7	5432.4
$m_{\tilde{\tau}_1}$	5097.3	5090.3	5757.6
$m_{\tilde{\tau}_2}$	5399.8	5386.1	5970.8
$m_{\tilde{\nu}_\tau}$	5373.3	5358.9	5933.1
$m_{\widetilde{W}_2}$	1132.3	1026.4	1178.5
$m_{\widetilde{W}_1}$	157.7	157.5	157.6
$m_{\widetilde{Z}_4}$	1144.4	1038.5	1187.5
$m_{\widetilde{Z}_3}$	674.0	537.6	773.7
$m_{\widetilde{Z}_2}$	156.8	157.3	156.5
$m_{\widetilde{Z}_1}$	148.5	147.3	148.8
m_h	124.3	124.2	124.3
$\Omega^{\rm std}_{\widetilde{Z}_1}h^2$	0.007	0.007	0.006
BF$(b\to s\gamma)\times 10^4$	3.1	3.1	3.1
BF$(B_s\to\mu^+\mu^-)\times 10^9$	3.8	3.8	3.8
$\sigma^{\rm SI}(\widetilde{Z}_1,p)$ (pb)	1.1×10^{-9}	1.5×10^{-9}	9.1×10^{-10}
$\sigma^{\rm SD}(\widetilde{Z}_1p)$ (pb)	3.6×10^{-5}	5.6×10^{-5}	3.2×10^{-5}
$\langle\sigma v\rangle\vert_{v\to 0}$ (cm^3/sec)	3.0×10^{-25}	3.0×10^{-25}	3.0×10^{-25}
$\Delta_{\rm EW}$	11.8	26.2	17.6

Table 1. Input parameters and masses in GeV units for a natural mini-landscape SUSY benchmark point as compared to a similar point with gaugino mass unification from the NUHM3 model. For the NUHM3 case we take $m_0(1,2) = 12.6$ TeV, $m_0(3) = 5360$ GeV, $m_{1/2} = 1176$ GeV, $A_0 = -7452$ GeV. Also shown is the spectrum for a second mini-landscape point with $m_{3/2} = 20$ TeV and $\alpha = 10$. We take $m_t = 173.2$ GeV.

Higgs mass at 124.3 GeV is in accord with its measured value if one allows for a ± 2 GeV theory error in the Isajet computation of m_h. The value of $\Delta_{\rm EW} = 11.8$ or $\Delta^{-1}_{\rm EW} = 8.5\%$ fine-tuning. Thus, the spectrum of the mini1 benchmark model is very natural and the

JHEP06(2017)101

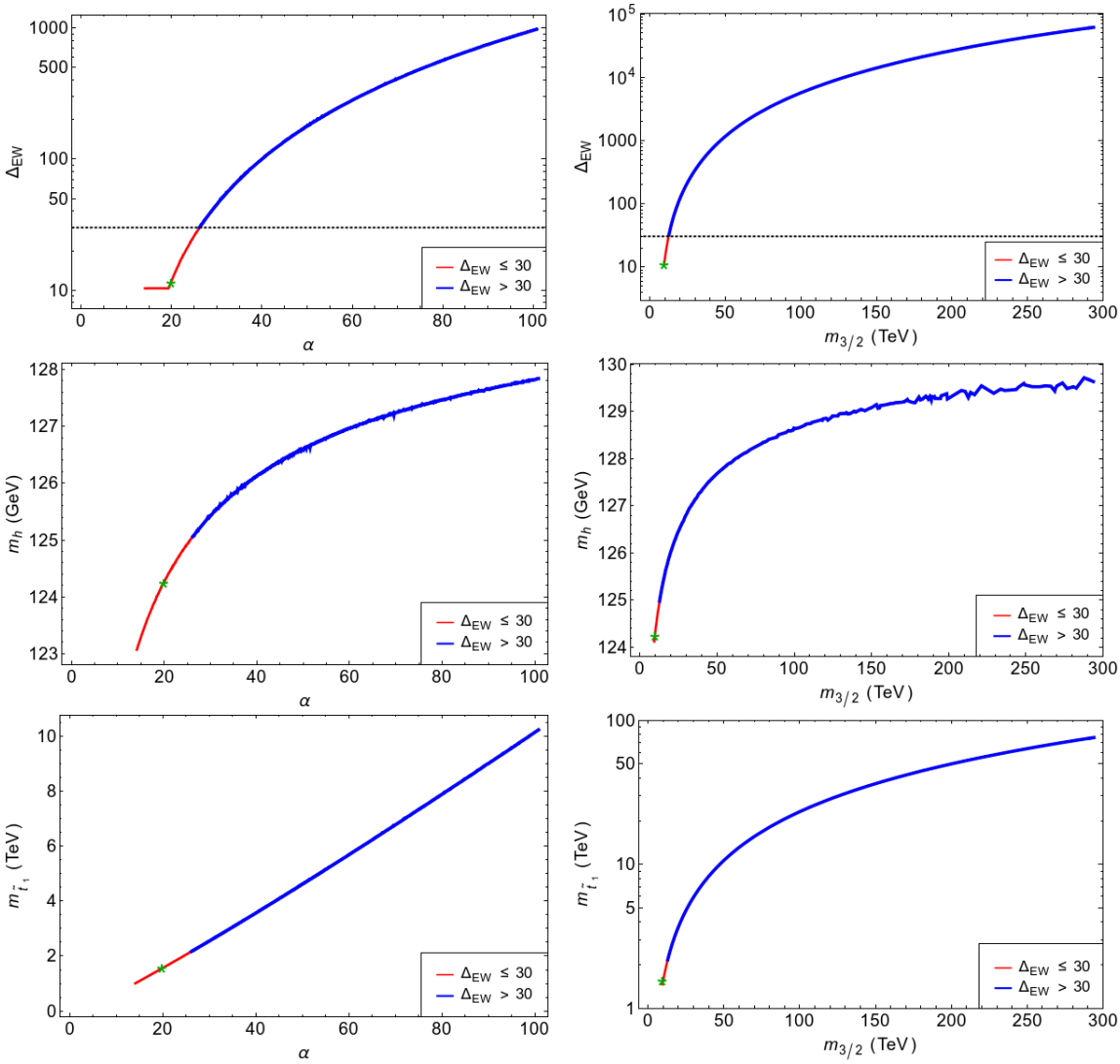

Figure 2. $\Delta_{\rm EW}$, m_h and $m_{\tilde{t}_1}$ vs. variation in α and $m_{3/2}$ for the mini1 benchmark point. The red portion of the curves has $\Delta_{\rm EW} < 30$. The green star denotes the mini1 benchmark point.

underlying string model that results in the mini-landscape picture with the chosen values of c_{m3} and a_3 would yield a natural high scale theory. The thermally-produced (TP) relic density of higgsino-like WIMPs comes in at $\Omega^{\rm TP}_{\widetilde{Z}_1}h^2 = 0.007$, below the measured value by a factor 17. The remainder may be made up by other particles: since we also insist on naturalness in the QCD sector, the QCD axion is the likely candidate. The relic abundance of both the QCD axion and higgsino-like WIMPs depends on various parameters from the Peccei-Quinn sector (axino and saxion mass, axion mis-alignment angle, axion decay constant f_a etc.) [90].

To see how aspects of the mini1 benchmark point depend on α and $m_{3/2}$, we show in figure 2 the variation in $\Delta_{\rm EW}$, m_h and $m_{\tilde{t}_1}$ versus α (left-column) and versus $m_{3/2}$ (right-column) where other parameters remain fixed at their mini1 BM values. The corresponding

JHEP06(2017)101

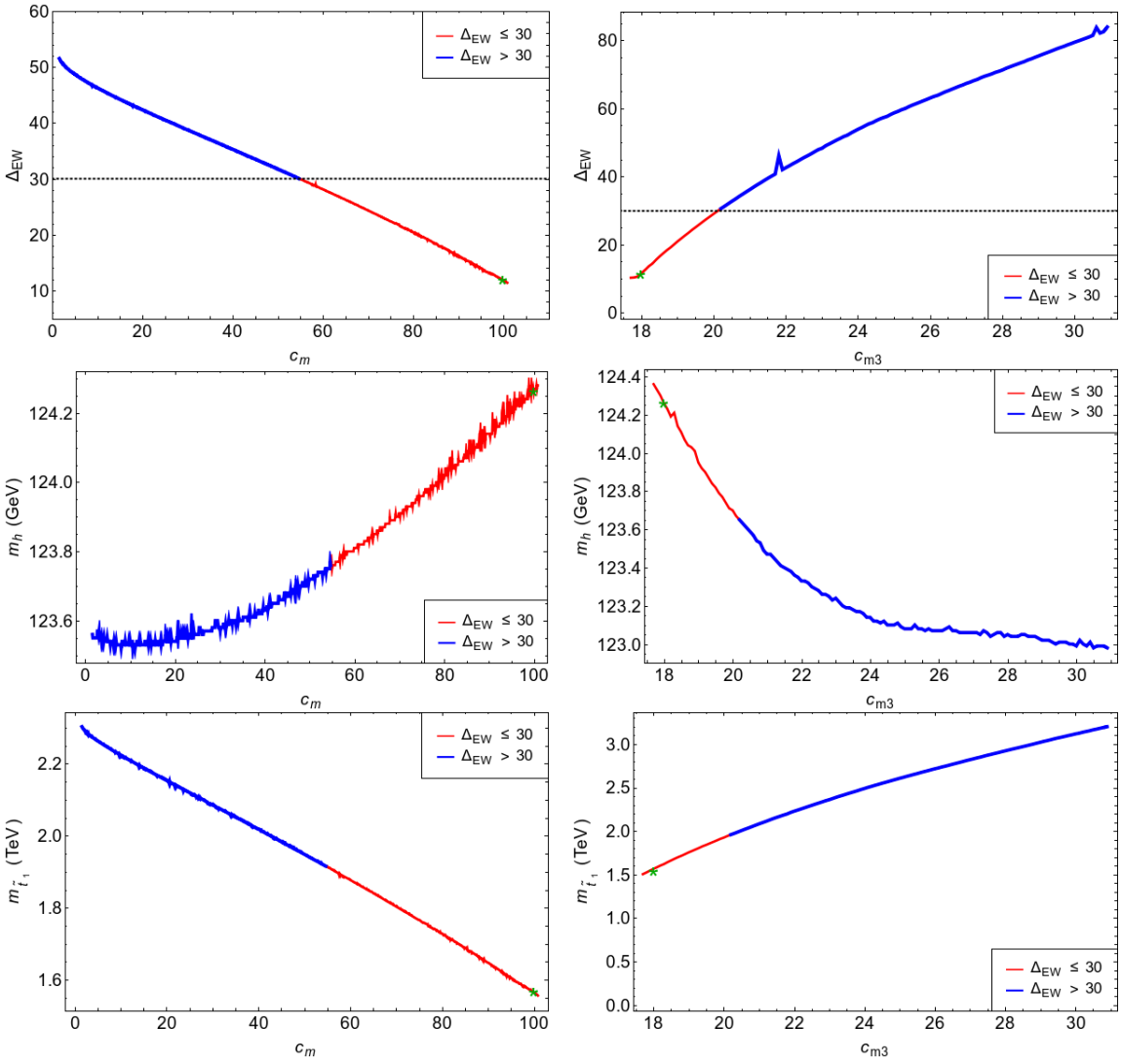

Figure 3. $\Delta_{\rm EW}$, m_h and $m_{\tilde{t}_1}$ vs. variation in c_m and c_{m3} for the mini1 benchmark point. The red portion of the curves has $\Delta_{\rm EW} < 30$. The green star denotes the mini1 benchmark point.

gluino mass can be inferred from figure 1 while the higgsino masses are $\sim |\mu|$. Other sfermions are typically too heavy to be produced at LHC14. The red portion of the curves has $\Delta_{\rm EW} < 30$ and the mini1 BM point is marked by the green cross. In the upper left frame, we see that $\Delta_{\rm EW}$ rises rapidly with increasing α since the superpartners (most notably the stops and gluino) become too heavy and the spectrum becomes unnatural, even with μ fixed at 150 GeV. This is due to the increasing values of radiative corrections, mainly $\Sigma_u^u(\tilde{t}_{1,2})$ in eq. (2.1). Also, m_h and $m_{\tilde{t}_1}$ rise with increasing α as the top squarks become increasingly heavy. Likewise, in the right column, we see $\Delta_{\rm EW}$ rapidly increases with increasing $m_{3/2}$, as do m_h and $m_{\tilde{t}_1}$. This is again due to rapidly increasing sparticle masses.

In figure 3, we show variation in $\Delta_{\rm EW}$, m_h and $m_{\tilde{t}_1}$ versus c_m (left-column) and c_{m3} (right-column), this time holding α and $m_{3/2}$ fixed at their mini1 benchmark values. From

JHEP06(2017)101

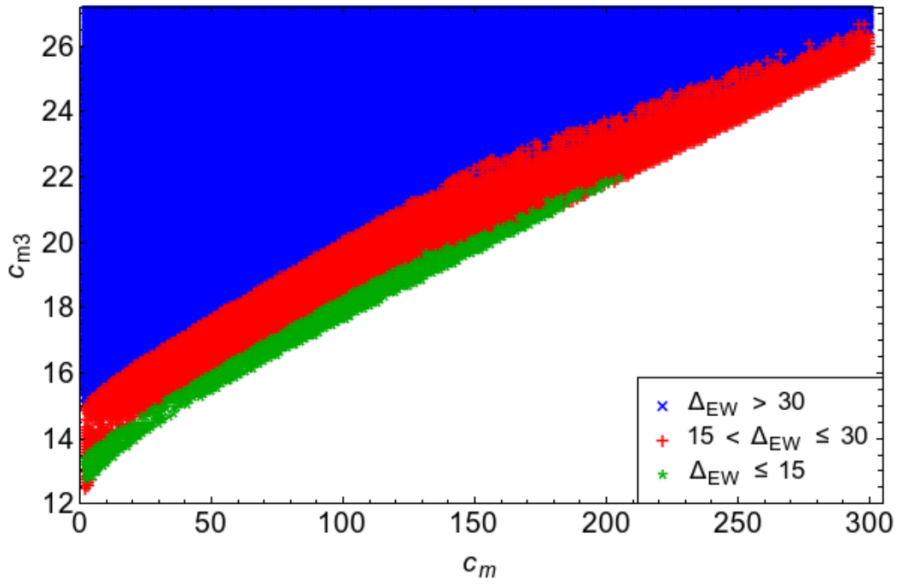

Figure 4. Allowed (colored) points in c_{m3} vs. c_m plane.

the upper-left frame, we see that $\Delta_{\rm EW}$ rapidly *drops* with increasing c_m. At first thought, one might not expect such sensitivity since c_m governs first/second generation scalar masses which seemingly have little to do with naturalness. However, long ago it has been emphasized that two-loop RG contributions [91] to scalar running become large for large first/second generation scalar soft terms (see [92] and more recently discussion in [38, 39]). These two loop RGE terms help drive the stop sector towards natural values as seen in the figure. As elaborated later, this same RG evolution also leads to a bound on the mini-landscape parameter space since too large values for first/second generation scalars drive third generation soft mass parameters tachyonic, leading to charge and color breaking (CCB) minima in the scalar potential. For the mini1 BM point, viable spectra are only generated out to $c_m \sim 100$, comfortably containing the $\Delta_{\rm EW} \leq 30$ region. In the right-column of figure 3, we show how the same quantities vary versus c_{m3}. As c_{m3} drops to values below ~ 17.5, some top squark soft mass parameters are driven tachyonic leading to CCB minima. Larger values of c_{m3} than are shown can be phenomenologically allowed, but only at an increasing cost to naturalness.

The interplay between the first/second and third generation scalar masses is illustrated in the c_{m3} vs. c_m plane shown in figure 4, with other parameters fixed to their mini1 BM values. We see again that as c_m increases (for fixed c_{m3}), the model becomes increasingly *natural* as exhibited by lower values of $\Delta_{\rm EW}$ dropping below 15. For yet higher c_m values, solutions are rejected due to CCB minima mentioned above. Also, as c_{m3} drops, the solutions become increasingly natural. The dividing line between natural (green) and forbidden (unshaded) solutions corresponds to *barely-broken* electroweak symmetry which is the essence of SUSY EW naturalness. In refs. [93] and [77], it is noted that large c_m solutions may be favoured by a string theory landscape which prefers large soft terms, consistent with the anthropic weak scale requirement $m_{W,Z,h} \sim 100\,{\rm GeV}$.

JHEP06(2017)101

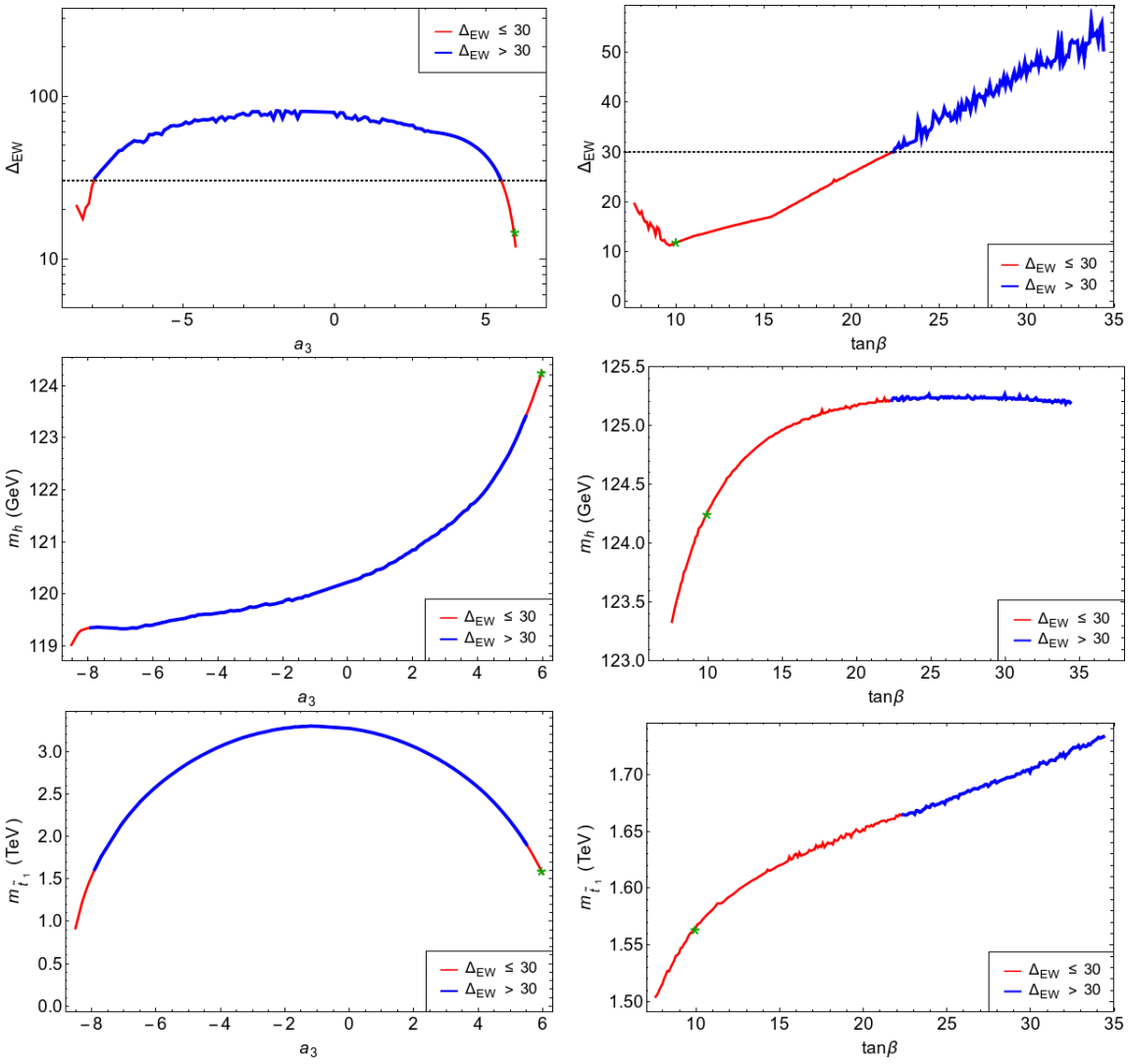

Figure 5. $\Delta_{\rm EW}$, m_h and $m_{\tilde{t}_1}$ vs. variation in a_3 and $\tan\beta$ for the mini1 benchmark point. The red portion of the curves has $\Delta_{\rm EW} < 30$. The green star denotes the mini1 benchmark point.

In figure 5, we show variation of $\Delta_{\rm EW}$, m_h and $m_{\tilde{t}_1}$ versus a_3 (left-column) and $\tan\beta$ (right-column). For much of the range of a_3, which dictates the magnitude of the trilinear soft terms $A_{t,b,\tau}$, the solutions are relatively unnatural and the value of m_h is too low. For large $a_3 \sim 5$–6, both the mixing in the stop sector and radiative corrections to m_h increase, leading to $m_h \sim 125\,{\rm GeV}$ whilst simultaneously reducing $\Delta_{\rm EW} < 30$. The value of m_h decreases for negative values of a_3 because $A_t({\rm weak}) \sim 1\,{\rm TeV}$ for $a_3 < -6$ to be compared with $A_t({\rm weak}) \sim -4\,{\rm TeV}$ at the right end of the plot. The value of $m_{\tilde{t}_1}$ gets reduced for values of a_3 consistent with both naturalness as well as the observed value of m_h. For large negative a_3, the value of $\Delta_{\rm EW}$ also drops below 30, but in this case m_h remains around 119 GeV. From the right-column, we see that low $\Delta_{\rm EW}$ prefers low $\tan\beta \lesssim 25$. For higher $\tan\beta$, then the b-quark Yukawa increases and the $\Sigma_u^u(\tilde{b}_{1,2})$ terms can contribute large values to $\Delta_{\rm EW}$ because the bottom squarks are typically heavier than the stops.

JHEP06(2017)101

4 Scan over natural mini-landscape parameter space

In this section, we present results from a scan over the portion of natural GMM parameter space which is in accord with expectations from the mini-landscape. To facilitate the scanning, we first restrict the high scale soft scalar mass parameters for the first two generations (recall these have no protection from extended supersymmetry in 4D) to be very close to $m_{3/2}$. Assuming that modulus-mediated contributions dominate the soft terms, we expect,

$$c_m \simeq (16\pi^2/\alpha)^2. \tag{4.1}$$

(In section 4.2 below we will examine how our results vary if we relax this assumption.) Further, we will define $m_0(1,2)$ and $m_0(3)$ as the average of first/second and third generation matter scalars at the GUT scale.

4.1 Results for $m_0(1,2) \simeq m_{3/2}$

As mentioned, to begin our analysis we first present results taking first/second generation SUSY breaking mass parameters close to the gravitino mass, and scan over

- α: 2–40,
- $m_{3/2}$: 3–65 TeV,
- c_m: fixed at $(16\pi^2/\alpha)^2$ so that $m_0(1,2) \simeq m_{3/2}$,
- c_{m3}: $1 - \min[40, (c_m/4)]$
- a_3: 1–12 in order to lift $m_h \sim 125$ GeV,
- $\tan\beta$: 3–60,
- μ: 100–360 GeV (lower bound to enforce LEP2 chargino search limits while upper limit from naturalness requiring $\Delta_{\rm EW} < 30$),
- m_A: 0.3–10 TeV.

In addition, we require of our solutions

- that there is an appropriate breakdown of EW symmetry (i.e. EW breaks but with no CCB minima),
- m_h: 123–127 GeV (allowing for $\sim \pm 2$ GeV theory error in our calculation of m_h),
- $m_{\tilde{g}} > 1.9$ TeV (in accord with recent LHC13 $\tilde{g}\tilde{g}$ search results),
- $m_{\tilde{t}_1} > 1$ TeV (in accord with recent LHC13 $\tilde{t}_1\bar{\tilde{t}}_1$ search results [94, 95]).

The results of our scan are shown in figure 6 where red points have $\Delta_{\rm EW} < 30$ while green points have $\Delta_{\rm EW} < 20$. From the plot we find an *upper bound* on $m_{3/2} \lesssim 24\,(32)$ TeV and $\Delta_{\rm EW} < 20\,(30)$. For higher $m_{3/2}$ values, first/second generation scalars are so heavy

JHEP06(2017)101

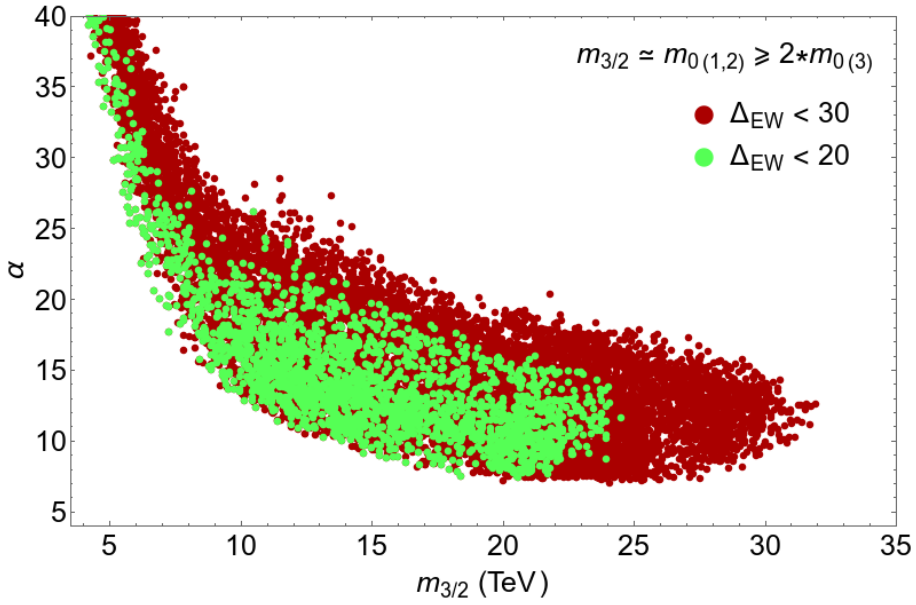

Figure 6. Allowed SUSY solutions in the α vs. $m_{3/2}$ plane of the natural mini-landscape model with other parameters scanned over as described in the text. We take $c_m = (16\pi^2/\alpha)^2$ and $c_{m3} < c_m/4$ to enforce $m_0(1,2) \simeq m_{3/2} \gtrsim 2m_0(3)$.

that some third generation scalars always are driven tachyonic leading to CCB minima. Since in the mini-landscape we expect $m_i(1,2) \sim m_{3/2} \sim \log(m_{\rm Pl}/m_{3/2}) \times m_j(3)$ then we really expect $m_{3/2} \gtrsim 5$–$10\,{\rm TeV}$.

The upper bound restricts the gravitino mass $m_{3/2} \lesssim 30\,{\rm TeV}$. This has three effects on phenomenology: 1. we expect first/second generation matter scalars to decouple from LHC searches, 2. the rather high first/second generation scalars suppress possible FCNC and CP-violating processes (offering at least a partial solution to the SUSY flavor and CP problems) [96], and 3. it softens the cosmological gravitino problem wherein thermal production of gravitinos followed by delayed decays can disrupt the successful predictions of Big Bang nucleosynthesis (in that heavier gravitinos decay more quickly and may then decay before the onset of BBN) [97, 98]. Note that in these models the moduli masses are expected to be $\sim \log(m_{\rm Pl}/m_{3/2})m_{3/2}$ so that for $m_{3/2} \sim 10$–$20\,{\rm TeV}$, then $m_T \sim 400$–$800\,{\rm TeV}$. Such heavy moduli decay relatively rapidly and thus evade the cosmological moduli problem.

A second result from figure 6 is that we obtain a lower bound on $\alpha \gtrsim 7$. This bound arises from the LHC bound on $m_{\tilde{g}}$ as can be seen from figure 1 It can be translated via eq. (1.1) into a *lower bound* on the mirage unification of $\mu_{\rm mir} \gtrsim 2.7 \times 10^{11}\,{\rm GeV}$. As a result, the weak scale gaugino spectrum is somewhat compressed, but gross compression is not possible. This is relevant for collider as well as for WIMP dark matter searches.

4.1.1 The mini2 benchmark model

From figure 6, we now readily pick out natural mini-landscape models with $m_{3/2} \sim 10$–$30\,{\rm TeV}$. A particular choice in shown in table 1 and labelled as *mini2*. The mini2

JHEP06(2017)101

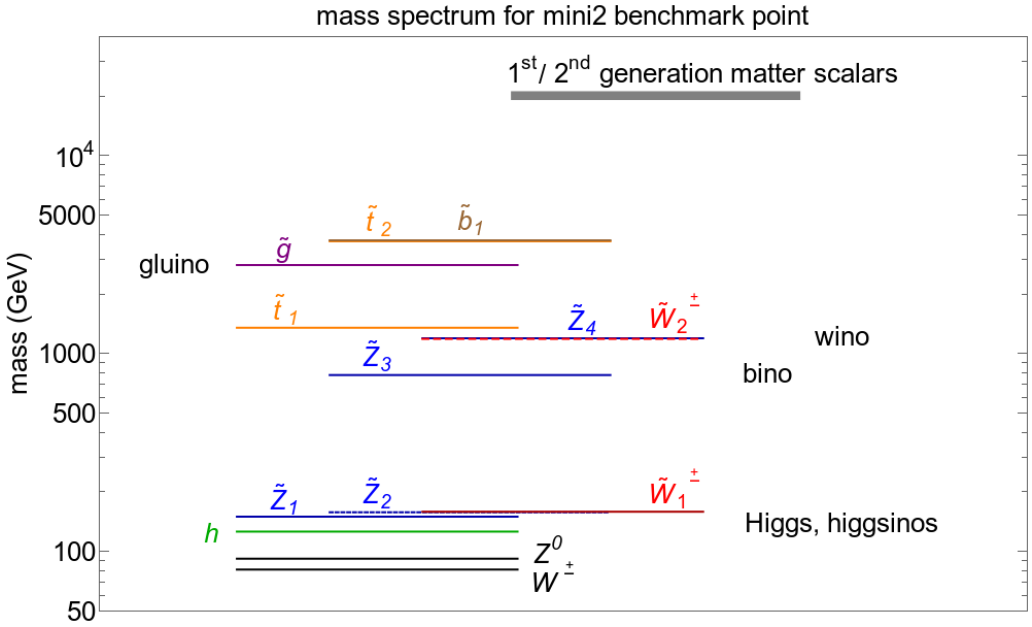

Figure 7. The superparticle mass spectra from the natural mini-landscape point mini2 of table 1.

benchmark point has $m_i(1,2) \simeq m_{3/2} = 20\,\text{TeV}$ while third generation scalars lie at $m_i(3) \sim 5\,\text{TeV}$. The light stop mass is suppressed both by renormalization effects from 1. the large top Yukawa coupling and 2. large first/second generation scalar masses as well as 3. by large intragenerational mixing: thus, $m_{\tilde{t}_1} = 1341.7\,\text{GeV}$, nearly at the maximal reach of HL-LHC [100]. The gluino mass is also close to the ultimate reach of HL-LHC. And yet the model is quite natural with $\Delta_{\text{EW}} = 17.6$. Indeed, natural SUSY models beyond the LHC reach are not difficult to find. The light higgsinos though would be easily accessible to ILC. The spectrum from the mini2 benchmark model point is illustrated in figure 7.

In figure 8 we show the evolution of gaugino masses from the mini2 benchmark point. In this case, the mirage scale is clearly seen at $\mu_{\text{mir}} \sim 10^{13}\,\text{GeV}$ resulting in a mild compression of gauginos as compared to models with gaugino mass unification. Here, we find $M_2/M_1 \sim 1.5$ whereas -ino mass unification delivers $M_2/M_1 \sim 2$. Also, M_3/M_1 here is ~ 3.6 whereas unified models tend to yield $M_3/M_1 \sim 6$ (as in the NUHM3 BM point). In obtaining these ratios, one must use the bino mass $m_{\tilde{Z}_3}$ since for natural SUSY the $\widetilde{W}_1$, $\widetilde{Z}_{1,2}$ are all higgsino-like. Of course, smaller values of α yield a greater compression of the gaugino spectrum. We will return to this in section 4.2 where we allow for deviations from eq. (4.1).

In figure 9, we show the evolution of various soft scalar masses for the mini2 benchmark point. The first/second generation scalars lie at $\sim 20\,\text{TeV}$ and hardly run. Third generation scalars lie around 5 TeV. The Higgs sector parameter m_{H_u} starts somewhat heavier than this at $Q = m_{\text{GUT}}$ but is radiatively-driven to natural low values at $Q \sim m_{\text{weak}}$ (notice here that though $m^2_{H_u}$ does not run to a negative value, EWSB nonetheless occurs once the negative radiative corrections Σ^u_u are included). The μ parameter hardly evolves and

JHEP06(2017)101

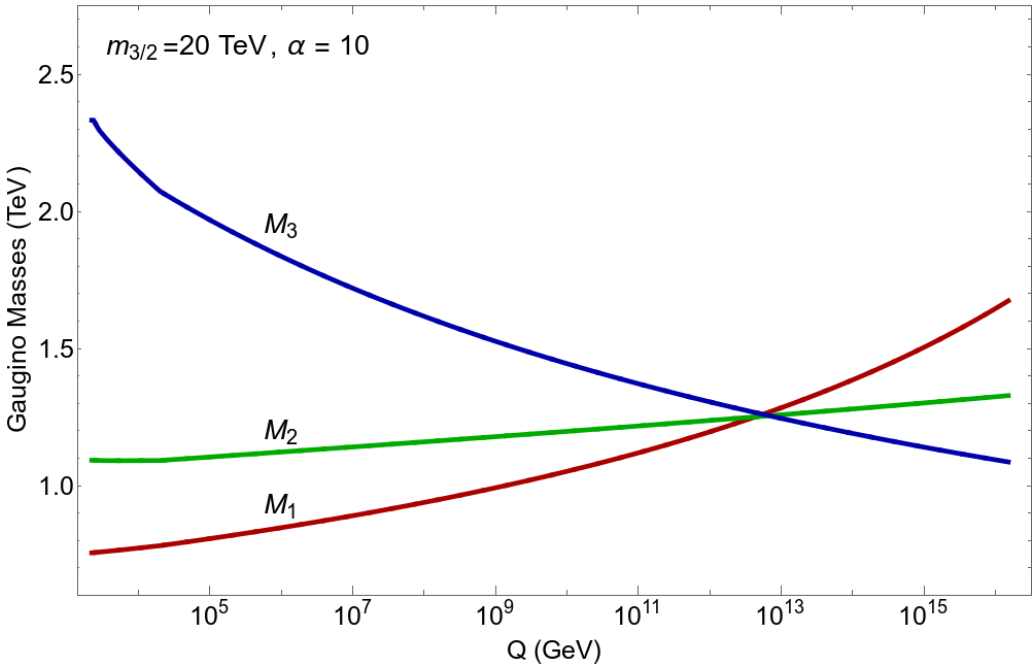

Figure 8. Evolution of gaugino masses from the mini2 benchmark point with $m_{3/2} = 20\,\text{TeV}$ and $\alpha = 10$.

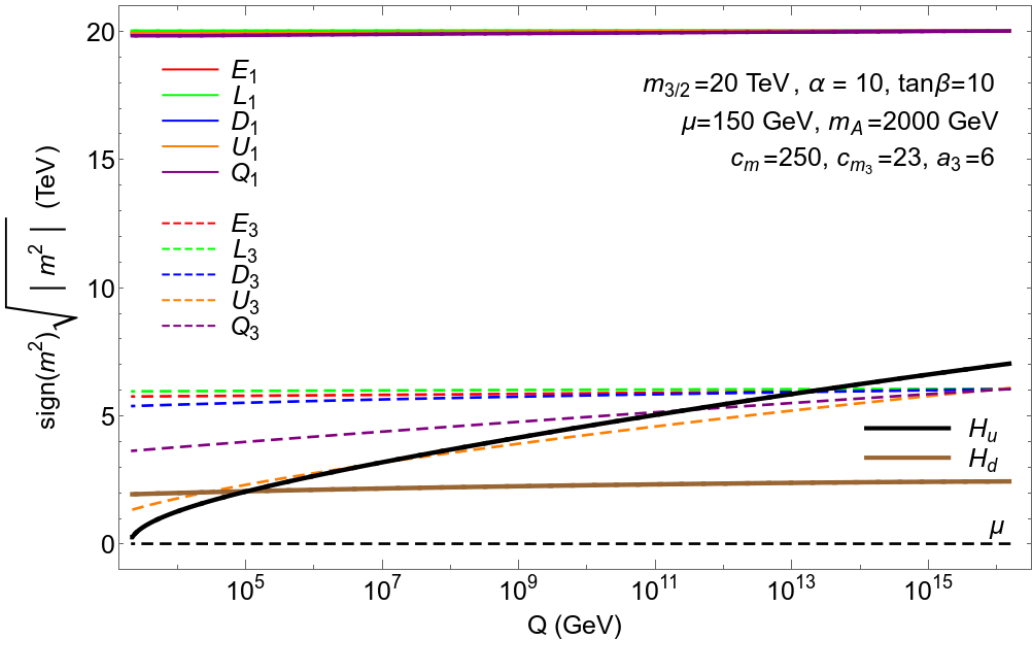

Figure 9. Plot of running scalar masses from the mini2 benchmark point with $m_{3/2} = 20\,\text{TeV}$, $\alpha = 10$, $\tan\beta = 10$ and $c_m = 250$, $a_3 = 6$ with $c_{m3} = 23$, $\mu = 150\,\text{GeV}$ and $m_A = 2\,\text{TeV}$ at the weak scale.

JHEP06(2017)101

lies around $\mu \sim 150\,\text{GeV}$. This figure illustrates well the three different physical scales: $\mu \sim m_{\text{weak}} \sim 100\,\text{GeV}$, $m(3,\text{Higgs}) \sim 5\,\text{TeV}$ and $m(1,2) \sim 20\,\text{TeV}$. We mention in passing that, in contrast to the earliest MM models, the scalar evolution does not exhibit any special feature at $Q = \mu_{\text{mir}}$.

4.2 Effect of relaxing $m_0(1,2) \simeq m_{3/2}$

In section 4.1, motivated by the fact that the the first and second generation sfermion mass parameters are less protected from SUSY breaking effects than the Higgs and top squark multiplets, we had fixed $m_0(1,2) \simeq m_{3/2}$. This led us, among other things, to conclude that the mirage scale could not be much lower than $\sim 10^{11}\,\text{GeV}$, with the associated mild compression of the gaugino spectrum. Depending on the details of the location of the first two generation fields, their SUSY breaking parameters may well be partially protected so that $m_0(1,2)$ are somewhat smaller than $m_{3/2}$ but, of course, still hierarchically separated from $m_0(3)$.

Motivated by this, we adopt a phenomenological attitude and perform other parameter scans, this time taking 1. $m_0(1,2) \simeq m_{3/2}/2$ and 2. $m_0(1,2) \simeq 2m_{3/2}$. We also require that $m_0(1,2) \geq 2m_0(3)$ (and $m_{3/2} \geq 2m_0(3)$ in case #2) to ensure that the hierarchy between generations remains as a feature of the mini-landscape. The scanned range of other parameters is the same as in figure 6. The solutions with Δ_{EW} from this generalized scans that also satisfy the LHC constraints are illustrated in figure 10. The blue dots show the same results as in figure 6. The gray dots show results for the case where $m_0(1,2) \simeq \frac{1}{2}m_{3/2}$ while the orange dots are for $m_0(1,2) \simeq 2m_{3/2}$. The main result is that for the case with smaller values of $m_0(1,2)$ shown by the gray dots, natural solutions with larger values of $m_{3/2}$ are allowed. This is not surprising if we recall that the upper limit on $m_{3/2}$ comes from the fact that the stop mass squared parameters become negative due to two loop contributions involving correspondingly heavy squarks in the first two generations. For a fixed gravitino mass, because $m_0(1,2)$ is about half as small for the gray points as compared with the blue points, it is clear that there will be viable solutions out to about twice larger gravitino masses in the gray point case. The situation is exactly reversed for the $m_0(1,2) = 2m_{3/2}$ case illustrated by the orange points.

An important phenomenological consequence of the large $m_{3/2}$ solutions is that they extend to α values as small as 4, to be compared with the bound $\alpha \gtrsim 7$ that we saw from figure 6. As a result, the mirage unification scale can be as low as $\sim 5 \times 10^7\,\text{GeV}$, with a concomitantly larger compression of gauginos[3] relative to the situation in figure 6. While our considerations emphasize that there is a *lower bound* on μ_{mir}, the precise value of this lower bound is sensitively dependent on just how small the ratio of $m_0(1,2)/m_{3/2}$ can be.

Before closing this discussion, we remind the reader that we were motivated to do the extended scan in figure 10 because the first two generations may well not be located exactly at the orbifold fixed point. In this case they may have some partial protection from SUSY breaking, resulting in soft terms smaller than $m_{3/2}$, but not as small as those of the stop

[3]For instance, for a natural point with $m_{3/2} = 50.6\,\text{TeV}$ and $\alpha = 4.3$ in the gray region, we have $M_1, M_2, M_3 = 1120, 1380, 2460\,\text{GeV}$, respectively at the weak scale.

JHEP06(2017)101

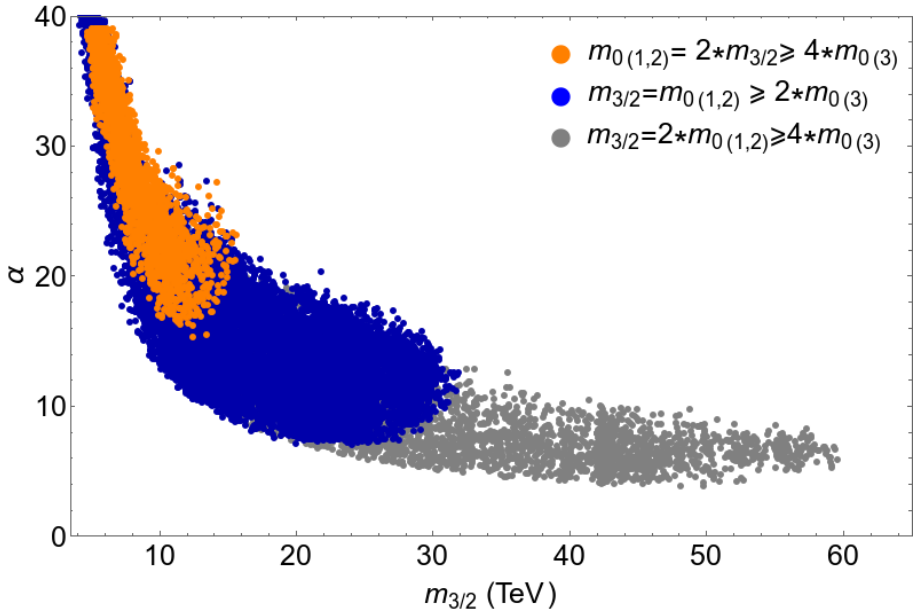

Figure 10. Allowed SUSY solutions with $\Delta_{\rm EW} < 30$ in the α vs. $m_{3/2}$ plane from an extended scan of the natural mini-landscape model with $c_m = 4 \times (16\pi^2/\alpha)^2$ to enforce $m_0(1,2) \simeq 2m_{3/2}$ (orange points), $c_m = (16\pi^2/\alpha)^2$ to enforce $m_0(1,2) \simeq m_{3/2}$ (blue points) and $c_m = \frac{1}{4}(16\pi^2/\alpha)^2$ to enforce $m_0(1,2) \simeq \frac{1}{2}m_{3/2}$ (gray points) as described in section 4.2 of the text. To maintain the hierarchy, we require $m_0(3) < \min[m_0(1,2)/2,\, m_{3/2}/2]$ in our scan. Other parameters scanned over as in figure 6. We note there are gray points not visible under the orange and blue dots extending down to low values of $m_{3/2}$.

and Higgs fields. From this perspective, the case with the orange dots is disfavoured in the mini-landscape picture. We have nonetheless shown it here for completeness.

5 Implications for LHC, ILC and dark matter searches

In this section, we investigate briefly the prospects for discovery of SUSY particles within the context of the natural mini-landscape picture. In this section, for brevity, all the results showing $\Delta_{\rm EW}$ versus the various sparticle masses are obtained for the canonical case with $c_m = (16\pi^2/\alpha)^2$, so that $m_0(1,2) \simeq m_{3/2}$, and requiring in addition that $m_0(1,2) \gtrsim 2m_0(3)$. These plots have been made by merging the results of a broad scan with those for a focussed scan for $\Delta_{\rm EW} < 30$, and the range of allowed values of μ is extended to 500 GeV.

5.1 Consequences for LHC and LHC33

We begin by showing results for the value of $\Delta_{\rm EW}$ vs. $m_{\tilde{t}_1}$ from our scan over mini-landscape parameter space in figure 11. We see that for $\Delta_{\rm EW} < 20$ we expect $m_{\tilde{t}_1} \lesssim 2$ TeV, while with the more conservative $\Delta_{\rm EW} < 30$ constraint $m_{\tilde{t}_1}$ may be as heavy as 2.5 TeV. For SUSY mass spectra from the natural mini-landscape where $m_{\widetilde{W}_1,\widetilde{Z}_{1,2}} \sim \mu \lesssim 200$–$300$ GeV, it has been found that $B(\tilde{t}_1 \to b\widetilde{W}_1) \sim 50\%$ while $B(\tilde{t}_1 \to t\widetilde{Z}_{1,2})$ are each at about 25% [99]. Meanwhile, the reach of LHC14 for top-squark pair production in several simplified models

JHEP06(2017)101

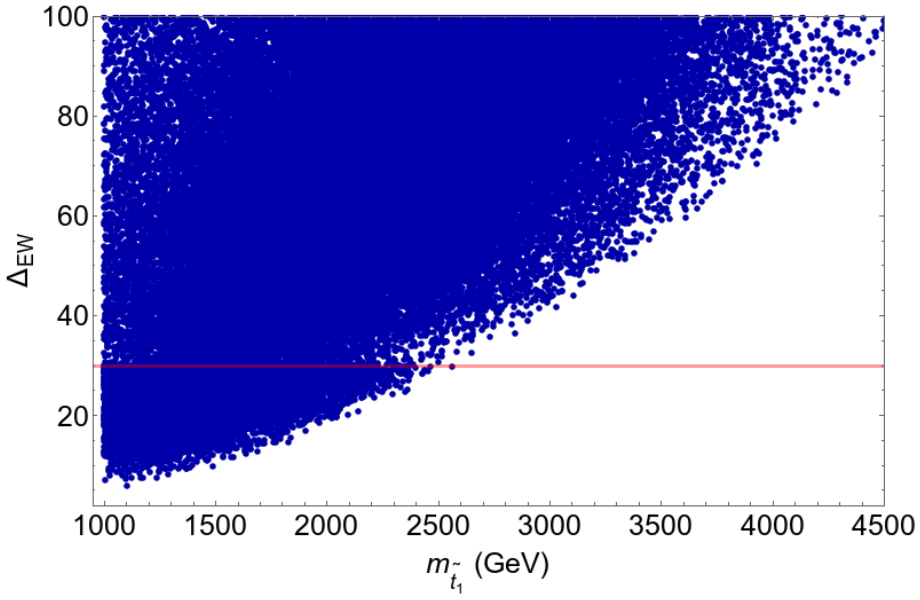

Figure 11. Plot of $\Delta_{\rm EW}$ vs. $m_{\tilde{t}_1}$ from a scan over natural mini-landscape parameter space with $m_0(1,2) \simeq m_{3/2}$.

has been calculated in ref. [100] and [101]. There, it was found that HL-LHC with $\sim 3\,{\rm ab}^{-1}$ of integrated luminosity, has a 5σ reach out to $m_{\tilde{t}_1} \sim 1.1$–$1.4\,{\rm TeV}$. Apparently HL-LHC will cover only a portion of mini-landscape parameter space via top squark pair searches. Assuming that the lighter top squark decays via $\tilde{t}_1 \to t\widetilde{Z}_{1,2}$ and $b\widetilde{W}_1$ with branching ratios $\simeq 0.25, 0.25$ and 0.5, respectively, the entire allowed range of top squark masses in figure 11 should be accessible at LHC33 where the stop reach extends to $m_{\tilde{t}_1} \sim 2.8\,{\rm TeV}$ for an integrated luminosity of $1\,{\rm ab}^{-1}$ [102].

In figure 12, we plot the value of $\Delta_{\rm EW}$ vs. $m_{\tilde{g}}$ from our scan over mini-landscape parameter space. For $\Delta_{\rm EW} < 20$, then $m_{\tilde{g}} \lesssim 4.5\,{\rm TeV}$ while the more conservative bound $\Delta_{\rm EW} < 30$ yields $m_{\tilde{g}} \lesssim 6\,{\rm TeV}$. The upper bound on $m_{\tilde{g}}$ from the mini-landscape model is higher than the value derived [104] from models such as NUHM2 where $m_0(1,2) = m_0(3)$. This is because in the mini-landscape case the positive contributions to stop masses from a heavy gluino (that lead to the upper bound on its mass) are partially compenstated by the large two-loop RGE contribution from heavy first/second generation scalars which depress the stop mass parameters. For the natural mini-landscape spectra, usually $\tilde{g} \to t\tilde{t}_1$ followed by $\tilde{t}_1$ decays as mentioned above. The reach of HL-LHC has been calculated for $pp \to \tilde{g}\tilde{g}X$ in ref. [103] where it was found that the 5σ reach of LHC with $0.3\,(3)\,{\rm ab}^{-1}$ extends to $m_{\tilde{g}} \sim 2.4\,(2.8)\,{\rm TeV}$. We see again that the HL-LHC will cover only a portion of natural mini-landscape parameter space via gluino pair searches. However, SUSY searches at LHC33 [88, 102] should be able to cover much of the gluino range in figure 12.

In figure 13 we plot the points from the general scans in figure 10 in the $m_{\tilde{t}_1} - m_{\tilde{g}}$ plane using the same color coding as before. We see that the upper bounds on the stop and gluino masses are insensitive to the precise value of $m_0(1,2)/m_{3/2}$. Since the gluino reach of LHC33 extends to $\sim 5.5\,{\rm TeV}$ if $m_{\tilde{t}_1} > 2\,{\rm TeV}$ [88], we conclude that LHC33 experiments

JHEP06(2017)101

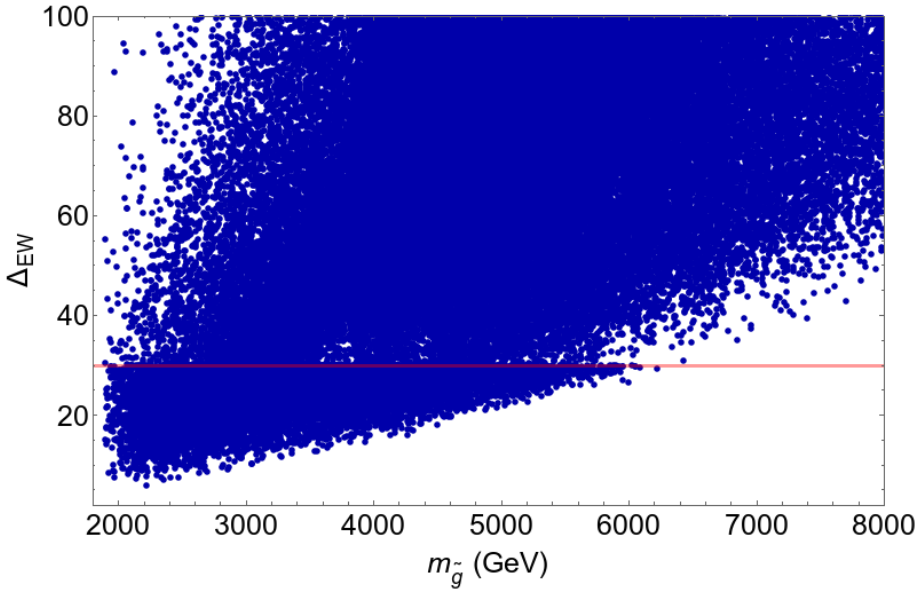

Figure 12. Plot of $\Delta_{\rm EW}$ vs. $m_{\tilde{g}}$ from a scan over natural mini-landscape parameter space with $m_0(1,2) \simeq m_{3/2}$.

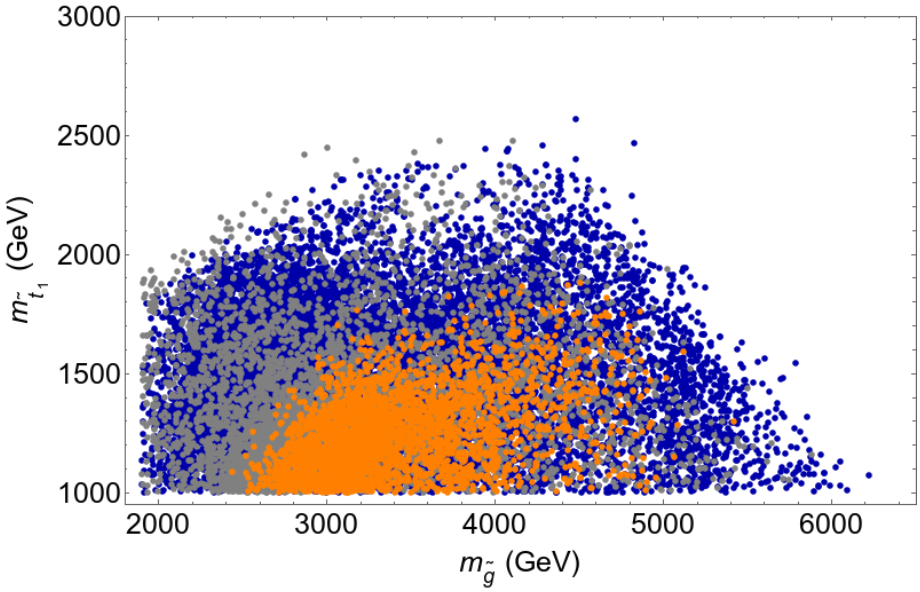

Figure 13. A scatter plot of $m_{\tilde{t}_1}$ versus $m_{\tilde{g}}$ for solutions with $\Delta_{\rm EW} < 30$ from the same three scans over the natural mini-landscape parameter space with $m_0(1,2) \simeq (2,1,1/2) \times m_{3/2}$ illustrated in figure 10. The color scheme in this figure is also the same as in figure 10.

should be sensitive to *both* gluino and squark signals over most of the natural parameter space of the mini-landscape framework, and of course, that SUSY will not evade detection at LHC33 if it is realized in this incarnation.

In figure 14, we plot $\Delta_{\rm EW}$ versus the value of the charged wino mass $m_{\widetilde{W}_2} \simeq M_2$(weak). We see that for $\Delta_{\rm EW} < 20\,(30)$ then $m_{\widetilde{W}_2}$ is bounded by $\sim 2\,(2.5)$ TeV. This is somewhat

JHEP06(2017)101

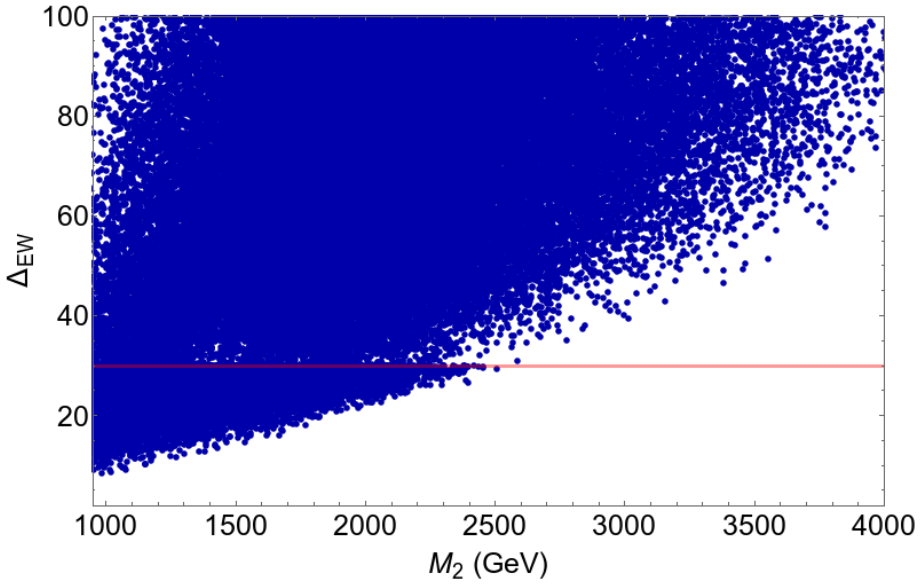

Figure 14. Plot of $\Delta_{\rm EW}$ vs. M_2(weak) from a scan over natural mini-landscape parameter space with $m_0(1,2) \simeq m_{3/2}$.

higher than the value obtained in models like NUHM2 with gaugino mass unification where instead it is found that $m_{\widetilde{W}_2} \lesssim 1.3\,(1.6)$ TeV [104]. The wino mass is relevant to LHC SUSY searches via the same-sign diboson channel where $pp \to \widetilde{W}_2\widetilde{Z}_4$ followed by $\widetilde{W}_2 \to W\widetilde{Z}_{1,2}$ and $\widetilde{Z}_4 \to W^{\pm}\widetilde{W}_1^{\mp}$. These decay modes lead about 50% of the time to a $W^{\pm}W^{\pm}+\not{E}_T$ final state which provides a low jet activity same-sign dilepton signature with very low SM backgrounds, the largest of which arises from $t\bar{t}W$ production. The LHC reach was estimated in this channel for 1 ab^{-1} to extend to $m_{1/2} \sim 1$ TeV corresponding to a reach in $m_{\widetilde{W}_2}$ of about 0.85 TeV [105, 106]. A rough extrapolation to 3 ab^{-1} should extend HL-LHC reach to the vicinity of $m_{\widetilde{W}_2} \sim 1.2$ TeV. In any case, again we see that HL-LHC can cover only a portion of natural mini-landscape parameter space via the SSdB signature.

In the natural mini-landscape model, we expect the higgsinos to have the tightest upper bounds from naturalness so that $m_{\widetilde{W}_1,\widetilde{Z}_{1,2}} \lesssim$ 200–300 GeV. While higgsino pair production can occur at large enough rates at LHC, the inter-higgsino mass gap is small, e.g. from figure 15, we see that $m_{\widetilde{Z}_2} - m_{\widetilde{Z}_1} \sim$ 3–15 GeV. As a result $\widetilde{Z}_2$, and analogously also $\widetilde{W}_1$, release very little visible energy in their decays, and so mainly contribute to the missing transverse energy. It has been shown that the resultant monojet signature from $pp \to \widetilde{Z}_{1,2}\widetilde{Z}_{1,2}j$ or $\widetilde{W}_1\widetilde{Z}_{1,2}j$ production at the LHC (where j denotes a hard QCD jet) occurs at only the 1–2% level above SM background from mainly Zj production where $Z \to \nu\bar{\nu}$ [107–109]. An alternative signature has been suggested [110, 111] where $pp \to \widetilde{Z}_1\widetilde{Z}_2 j$ production followed by $\widetilde{Z}_2 \to \ell^+\ell^-\widetilde{Z}_1$ giving rise to soft dileptons plus jet (used for trigger) plus $\not{E}_T$. The reach of HL-LHC in this channel has been found to extend to $\mu \sim 250$ GeV for mass gaps $\sim$ 10–20 GeV. In the case of the mini-landscape where bino and winos can be somewhat heavier than in unified gaugino mass models the inter-higgsino mass gap is typically smaller (less higgsino-gaugino mixing), as seen in figure 15.

JHEP06(2017)101

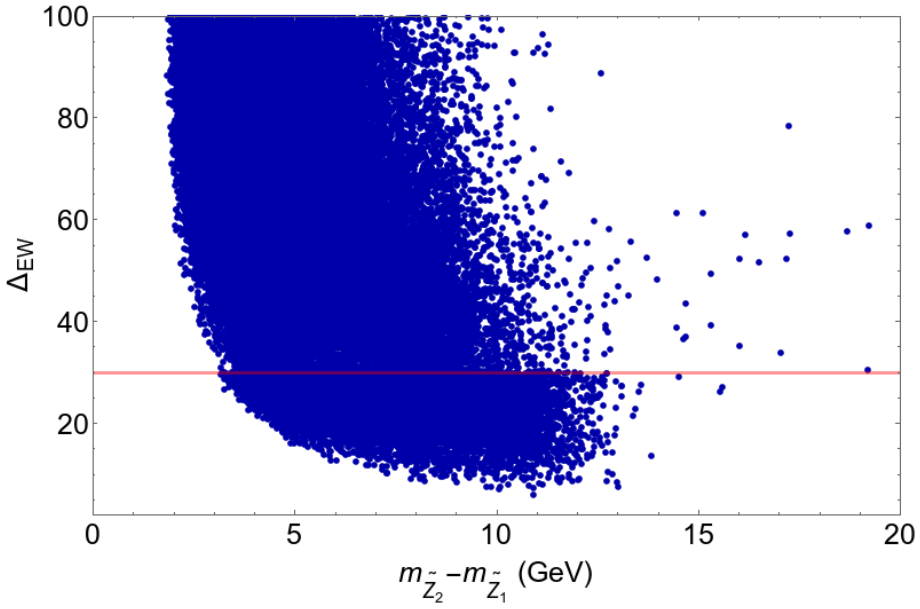

Figure 15. Plot of $\Delta_{\rm EW}$ vs. $m_{\tilde{Z}_2} - m_{\tilde{s}_1}$ from a scan over natural mini-landscape parameter space with $m_0(1,2) \simeq m_{3/2}$.

This makes detection of the $\ell^+\ell^- j + \not{E}_T$ channel somewhat more difficult than in models with gaugino mass unification both because the dilepton $p_T(\ell)$ spectra is softer and also because SM backgrounds from Drell-Yan and Υ and associated production become more relevant.

5.2 Consequences for ILC

The proposed International Linear e^+e^- Collider is proposed to be built in Japan and could operate initially at $\sqrt{s} \sim 250$ GeV as a Higgs factory with later upgrades to $\sqrt{s} = 500$ and even 1000 GeV. The light higgsinos $\widetilde{W}_1$ and $\widetilde{Z}_{1,2}$ are required to be not too far from $m_{W,Z,h}$ via the naturalness condition: see figure 16 where for $\Delta_{\rm EW} < 20\,(30)$, we have $m_{\widetilde{W}_1} \lesssim 300\,(375)$ GeV. This means that SUSY signals from $e^+e^- \to \widetilde{W}_1^+\widetilde{W}_1^-$ and $\widetilde{Z}_1\widetilde{Z}_2$ processes should be observable provided that these reactions are kinematically accessible. The modest inter-higgsino mass gaps probably offer no great obstacle to discovery of higgsino pair production in the clean environment of e^+e^- collisions [112–114], although detailed studies for mass gaps of $\sim$ 5–10 GeV have not yet been completed.

An additional benefit of $e^+e^- \to \widetilde{W}_1^+\widetilde{W}_1^-$ and $\widetilde{Z}_1\widetilde{Z}_2$ production is the precision measurements of $m_{\widetilde{W}_1}$, $m_{\widetilde{Z}_2}$ and $m_{\widetilde{Z}_1}$. These measurements shoud give high precision on the value of the superpotential μ parameter. Also, the inter-higgsino mass splitting is dependent on the values of the gaugino masses M_1 and M_2. From refs. [113] and [114], these ought to be extractable using fitting procedures. It would be interesting to carefully examine whether these methods that have been shown to provide useful measurements in a case study with a neutralino mass gap of 22 GeV continue to work for the smaller mass gaps of 3–15 GeV typical of the mini-landscape picture.

JHEP06(2017)101

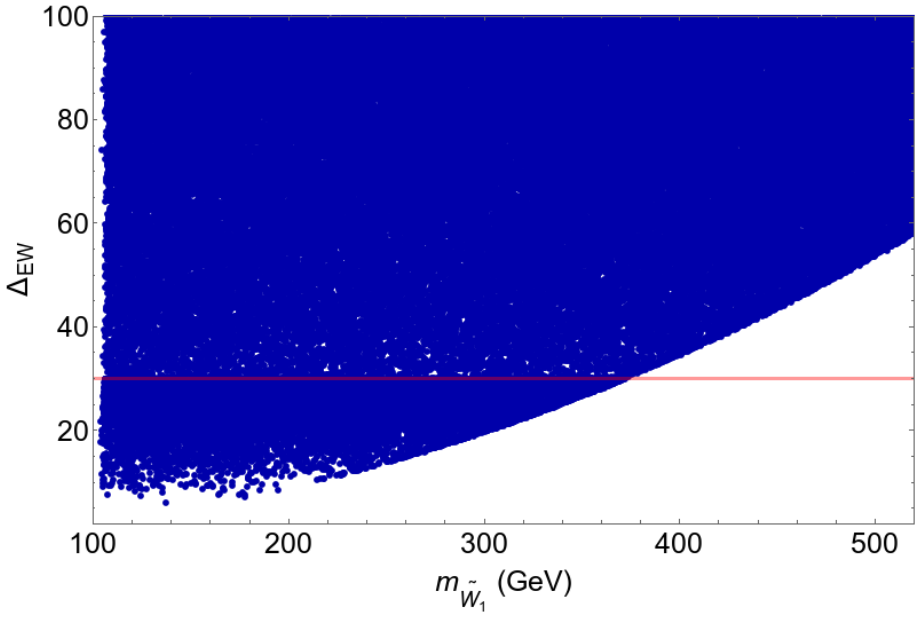

Figure 16. Plot of $\Delta_{\rm EW}$ vs. $m_{\widetilde{W}_1}$ from a scan over natural mini-landscape parameter space with $m_0(1,2) \simeq m_{3/2}$.

Once the gaugino masses are extracted (including M_3 if gluino pair production is found at LHC [103] or its energy upgrade) then one will be able to test if the gaugino masses unify at $Q = m_{\rm GUT}$, or at $Q = \mu_{\rm mir}$ as expected in the mini-landscape picture where the gaugino mass pattern is as given by mirage mediation.

5.3 Consequences for WIMP and axion searches

Dark matter in the natural mini-landscape framework is expected to occur as a mixture of QCD axions and higgsino-like WIMPs. The WIMPs are thermally underproduced owing to large higgsino-higgsino annihilation and co-annihilation reactions in the early universe. Typically the higgsino-like WIMP thermal abundance is a factor 10–20 below the measured value. Since it is reasonable to require naturalness in the QCD sector as well (solving the strong CP problem), the QCD axion is a highly motivated candidate for the remaining dark matter. The SUSY DFSZ axion has been suggested as a solution to the SUSY μ problem [75] while simultaneously allowing for a little hierarchy [76] $\mu \sim f_a^2/m_{\rm Pl} \ll m_{\rm SUSY} \sim \Lambda^3/m_{\rm Pl}^2$ where Λ is the scale for gaugino condensation occuring in the hidden sector.

While axions are produced as usual non-thermally via vacuum mis-alignment, one must also account for the other components of the axion superfield: the spin-1/2 axino $\tilde{a}$ and the spin-0 saxion s. Axinos and saxions are expected to acquire masses $\sim m_{3/2} \sim 10$–$50\,{\rm TeV}$. Axinos can be produced thermally and if they decay after WIMP freeze-out then they augment the WIMP abundance. Saxions can be produced thermally but also via coherent oscillations. If they decay after freeze-out, then they also may augment the WIMP abundance. If they decay dominantly to SM particles then they may inject late time entropy

JHEP06(2017)101

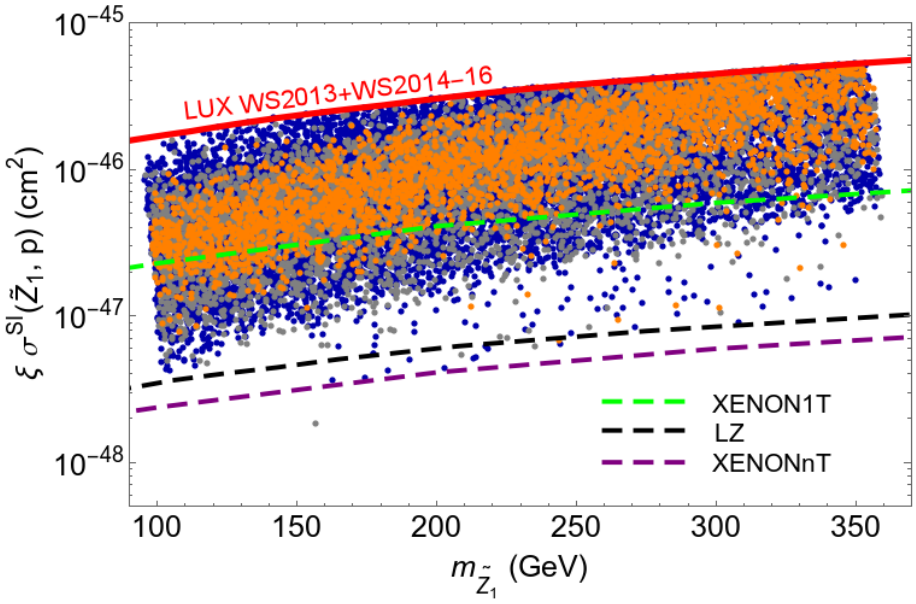

Figure 17. A scatter plot of $\xi\sigma^{\rm SI}(\widetilde{Z}_1, p)$ versus $m_{\widetilde{Z}1}$ for solutions with $\Delta_{\rm EW} < 30$ from the same three scans over the natural mini-landscape parameter space with $m_0(1,2) \simeq (2,1,1/2) \times m_{3/2}$ illustrated in figure 10. Here ξ is the higgsino fraction of the total CDM density, assuming that the relic density of higgsino WIMPs is given by its thermal value. The colour scheme in this figure is the same as in figure 10.

into the cosmic plasma thus diluting any relics which are present. And if they decay to axions $s \to aa$ then they may inject additional relativistic degrees of freedom in the cosmic plasma (for which there are strong bounds on additional neutrino species $\Delta N_{\rm eff} \lesssim 1$). The exact abundances of axions and higgsino-like WIMPs depends on the various PQ sector parameters and sample calculations are shown in the eight coupled Boltzmann equation solutions from ref. [115, 116]. It was found that for much of the allowed parameter space, axions dominate the relic abundance [90].

Prospects for higgsino-like WIMP direct detection via spin-independent (SI) or spin-dependent (SD) scattering have been shown in ref. [117] for a variety of models. A key point here is that the detection rates may be lowered by up to a factor $\xi \equiv \Omega_{\widetilde{Z}_1} h^2/0.12$ to account for the depleted local abundance of WIMPs from the usually assumed density $\rho_{\rm local} \simeq 0.3\,{\rm GeV/cm}^3$. The indirect WIMP detection rates from cosmic WIMP annihilation depend on the square of the WIMP density, and so are suppressed by a factor of ξ^2.

In figure 17, we show a plot of the expected scaled spin-independent WIMP-nucleon cross section for natural mini-landscape models assuming that the relic density of the higgsino-like WIMP is given by its thermal value. We show results for the same three scans from figure 10, using the same colour-coding as in this figure. We plot only those points consistent with the current bounds from the LUX experiment (with 95+332 live days combined exposure) [118]. The expected direct detection rates are not very sensitive to the ratio $m_0(1,2)/m_{3/2}$, assuming it is within a factor 2 of unity. We also show projections for the sensitivity of the XENON1T, XENONnT [119] and the LZ [120] experiments.

JHEP06(2017)101

In contrast to expectations in natural SUSY models with gaugino mass unification where it was concluded that XENON1T would be sensitive to the direct detection signal over the bulk of parameter space [117], we see that for the mini-landscape picture multi-ton detectors will be needed for complete coverage. This is because the bino and wino masses can be substantially larger in the mini-landscape picture compared to models with unified gaugino masses, reducing the gaugino content in the higgsino-like $\widetilde{Z}_1$. As a result, the $h\widetilde{Z}_1\widetilde{Z}_1$ coupling which arises only via gaugino-higgsino-Higgs boson interactions, is correspondingly reduced. Since WIMP-nucleon scattering is typically dominated by the h-exchange contribution, the direct detection cross section can decrease to smaller values in the mini-landscape picture. It is heartening though that future detectors such as LZ and XENONnT are projected to probe the entire natural mini-landscape parameter space subject to the usual caveats that there is no injection of entropy (from late decays of moduli or from the decays of saxions) that dilutes the WIMP density below its thermal value.

Turning to indirect detection, we have also evaluated expectations for detection of gamma ray signals from cosmic WIMP annihilation. We find that these are a factor of 10–20 below the current bounds from the Fermi-LAT/MAGIC collaboration [121], assuming WIMP annihilation to W^+W^- pairs. We also find that, except perhaps at the highest values of WIMP masses in the last figure, the gamma ray signals also lie beyond the reach of the CTA [122], assuming a 500 h exposure. We do not show these results for the sake of brevity.

6 Conclusions

In this paper, we have examined the superparticle mass spectra and broad phenomenological features of the mini-landscape picture, focussing on the region of parameter space consistent with electroweak naturalness. The mini-landscape scenario is a string-motivated construction based on the expectation that the MSSM emerges as the low energy theory in special regions of the string landscape. The salient feature of this scenario is that the multiplet structure as well as the masses of the MSSM fields depends on their location in the compactified manifold. The symmetry group of the low energy theory is just $G_{\rm SM}$, but first and second generation multiplets that live near the orbifold fixed point have enhanced symmetry and enter as complete representations of SO(10), while only the SM gauge, Higgs and third generation matter multiplets remain at lower energies. Superymmetry breaking is also felt differently by the various particles. Gaugino mass parameters are suppressed relative to $m_{3/2}$ and exhibit the mirage mediation pattern in eq. (2.5). Third generation squark and soft Higgs parameters are also relatively suppressed, while first/second generation soft SUSY breaking masses are expected to be comparable to $m_{3/2}$. The mini-landscape picture leads to the parametrization of soft SUSY breaking parameters given by eqs. (2.5)–(2.12) which we have dubbed generalized mirage mediation. This framework is completely specified by the parameter set (2.4).

We have identified the region of model parameter space consistent with low electroweak fine-tuning $\Delta_{\rm EW} \leq 30$. The $\Delta_{\rm EW}$ measure yields the most conservative value of fine tuning in the sense that it allows for the fact that soft SUSY breaking parameters — that are often

JHEP06(2017)101

regarded as independent — may actually be correlated by the SUSY breaking mechanism. The main features of the superparticle spectra in this preferred region are summarized below and compared to corresponding features of the natural NUHM2 model where gaugino mass unification is assumed.

- As in all models with low electroweak fine-tuning, we expect light higgsino states $\widetilde{Z}_{1,2}, \widetilde{W}_1^{\pm}$ with masses not far above m_Z. In the mini-landscape scenario, the neutral higgsino mass splitting is typically 3–15 GeV (to be compared with 10–25 GeV in the natural NUHM2 model [104]).

- In contrast to the NUHM2 model where gaugino mass unification leads to weak scale gaugino masses in the ratio $M_1 : M_2 : M_3 \simeq 1 : 2 : 6$, the gaugino spectrum from the natural mini-landscape may be compressed. The degree of compression sensitively depends on the mirage unification scale $\mu_{\rm mir}$ which in turn depends on how low α can be while maintaining consistency with LHC bounds on $m_{\tilde{g}}$. This compression is relatively mild if we assume the squark mass parameters of the first two generations are close to $m_{3/2}$ but significantly larger compression is possible if these squarks are much lighter than $m_{3/2}$.

- We find that $m_{\tilde{g}} \lesssim 6\,{\rm TeV}$ and $m_{\tilde{t}_1} \lesssim 2.5\,{\rm TeV}$ if $\Delta_{\rm EW} < 30$ and $m_0(1,2)$ is within a factor 2 of $m_{3/2}$. Moreover, $m_{\tilde{g}} > 5\,{\rm TeV}$ only when $m_{\tilde{t}_1} < 2\,{\rm TeV}$.

- The first two generations of squarks and sleptons are very heavy. While this puts them well beyond the range of LHC, it also ameliorates the SUSY flavour problem.

While it is possible that experiments at the LHC may discover the gluino or the top squark if SUSY is realized in the natural region of mini-landscape parameters, their discovery is not guaranteed at even the HL-LHC. Moreover, the discovery of SUSY via $W^{\pm}W^{\pm}+\not{E}_T$ events which is nearly guaranteed at the HL-LHC in the natural NUHM2 model, is no longer a sure thing within the mini-landscape picture because the compression of the gaugino spectrum now allows much heavier winos even in natural models. This same compression also leads to a reduced mass difference $m_{\widetilde{Z}_2} - m_{\widetilde{Z}_1}$ rendering the mono-jet plus soft dilepton signal (which was observable in the natural NUHM2 model) more difficult to extract. We are thus forced to conclude that SUSY detection is not guaranteed over the entire natural parameter space of the mini-landscape model even at the HL-LHC. Detection of higgsino-like WIMPs at XENON1T is also not guaranteed in the mini-landscape picture. Larger detectors such as XENONnT and LZ will, however cover the entire natural mini-landscape parameter space unless late injection of entropy reduces the WIMP density from what we expect assuming that the higgsino is a thermally produced relic in standard Big Bang cosmology.

Turning to future colliders, it is very likely that experiments at electron positron colliders will be able to detect higgsinos via $e^+e^- \to \widetilde{Z}_1\widetilde{Z}_2, \widetilde{W}_1^+\widetilde{W}_1^-$ production if these reactions are kinematically accessible. Experiments at LHC33 will be able to access top squark signals over the entire natural SUSY mass range, and also gluino signals over almost all of the natural range of $m_{\tilde{g}}$ in the mini-landscape scenario.

JHEP06(2017)101

Acknowledgments

We thank Peter Nilles for several communications and clarifications about the mini-landscape scenario. We thank Werner Porod for checking our GMM boundary conditions using Spheno. This work was supported in part by the US Department of Energy, Office of High Energy Physics. The computing for this project was performed at the OU Supercomputing Center for Education & Research (OSCER) at the University of Oklahoma (OU).

JHEP06(2017)101

References

[1] A.N. Schellekens, *Life at the interface of particle physics and string theory*, *Rev. Mod. Phys.* **85** (2013) 1491 [arXiv:1306.5083] [INSPIRE].

[2] K.R. Dienes, *String theory and the path to unification: a review of recent developments*, *Phys. Rept.* **287** (1997) 447 [hep-th/9602045] [INSPIRE].

[3] K.R. Dienes, *The string landscape: a personal perspective*, *Adv. Ser. Direct. High Energy Phys.* **22** (2015) 81 [INSPIRE].

[4] H.P. Nilles and P.K.S. Vaudrevange, *Geography of fields in extra dimensions: string theory lessons for particle physics*, *Adv. Ser. Direct. High Energy Phys.* **22** (2015) 49 [INSPIRE].

[5] E. Witten, *Dynamical breaking of supersymmetry*, *Nucl. Phys.* **B 188** (1981) 513 [INSPIRE].

[6] E. Witten, *Mass hierarchies in supersymmetric theories*, *Phys. Lett.* **B 105** (1981) 267 [INSPIRE].

[7] R.K. Kaul, *Gauge hierarchy in a supersymmetric model*, *Phys. Lett.* **B 109** (1982) 19 [INSPIRE].

[8] S. Dimopoulos, S. Raby and F. Wilczek, *Supersymmetry and the scale of unification*, *Phys. Rev.* **D 24** (1981) 1681 [INSPIRE].

[9] U. Amaldi, W. de Boer and H. Furstenau, *Comparison of grand unified theories with electroweak and strong coupling constants measured at LEP*, *Phys. Lett.* **B 260** (1991) 447 [INSPIRE].

[10] J.R. Ellis, S. Kelley and D.V. Nanopoulos, *Probing the desert using gauge coupling unification*, *Phys. Lett.* **B 260** (1991) 131 [INSPIRE].

[11] P. Langacker and M.-x. Luo, *Implications of precision electroweak experiments for M_t, ρ_0, $\sin^2\theta_W$ and grand unification*, *Phys. Rev.* **D 44** (1991) 817 [INSPIRE].

[12] L.E. Ibáñez and G.G. Ross, $SU(2)_L \times U(1)$ *symmetry breaking as a radiative effect of supersymmetry breaking in guts*, *Phys. Lett.* **B 110** (1982) 215 [INSPIRE].

[13] K. Inoue, A. Kakuto, H. Komatsu and S. Takeshita, *Aspects of grand unified models with softly broken supersymmetry*, *Prog. Theor. Phys.* **68** (1982) 927 [*Erratum ibid.* **70** (1983) 330] [INSPIRE].

[14] K. Inoue, A. Kakuto, H. Komatsu and S. Takeshita, *Renormalization of supersymmetry breaking parameters revisited*, *Prog. Theor. Phys.* **71** (1984) 413 [INSPIRE].

[15] L.E. Ibáñez, *Locally supersymmetric* SU(5) *grand unification*, *Phys. Lett.* **B 118** (1982) 73 [INSPIRE].

[16] H.P. Nilles, M. Srednicki and D. Wyler, *Weak interaction breakdown induced by supergravity*, *Phys. Lett.* **B 120** (1983) 346 [INSPIRE].

[17] J.R. Ellis, J.S. Hagelin, D.V. Nanopoulos and K. Tamvakis, *Weak symmetry breaking by radiative corrections in broken supergravity*, *Phys. Lett.* **B 125** (1983) 275 [INSPIRE].

[18] L. Álvarez-Gaumé, J. Polchinski and M.B. Wise, *Minimal low-energy supergravity*, *Nucl. Phys.* **B 221** (1983) 495 [INSPIRE].

[19] B.A. Ovrut and S. Raby, *The locally supersymmetric geometrical hierarchy model*, *Phys. Lett.* **B 130** (1983) 277 [INSPIRE].

[20] L.E. Ibáñez and G.G. Ross, *Supersymmetric Higgs and radiative electroweak breaking*, *C. R. Phys.* **8** (2007) 1013 [hep-ph/0702046] [INSPIRE].

[21] ATLAS collaboration, *Observation of a new particle in the search for the standard model Higgs boson with the ATLAS detector at the LHC*, *Phys. Lett.* **B 716** (2012) 1 [arXiv:1207.7214] [INSPIRE].

[22] CMS collaboration, *Observation of a new boson at a mass of 125 GeV with the CMS experiment at the LHC*, *Phys. Lett.* **B 716** (2012) 30 [arXiv:1207.7235] [INSPIRE].

[23] H.E. Haber and R. Hempfling, *Can the mass of the lightest Higgs boson of the minimal supersymmetric model be larger than m_Z?*, *Phys. Rev. Lett.* **66** (1991) 1815 [INSPIRE].

[24] J.R. Ellis, G. Ridolfi and F. Zwirner, *Radiative corrections to the masses of supersymmetric Higgs bosons*, *Phys. Lett.* **B 257** (1991) 83 [INSPIRE].

[25] Y. Okada, M. Yamaguchi and T. Yanagida, *Upper bound of the lightest Higgs boson mass in the minimal supersymmetric standard model*, *Prog. Theor. Phys.* **85** (1991) 1 [INSPIRE].

[26] M. Carena and H.E. Haber, *Higgs boson theory and phenomenology*, *Prog. Part. Nucl. Phys.* **50** (2003) 63 [hep-ph/0208209] [INSPIRE].

[27] G. Cleaver, M. Cvetič, J.R. Espinosa, L.L. Everett and P. Langacker, *Flat directions in three generation free fermionic string models*, *Nucl. Phys.* **B 545** (1999) 47 [hep-th/9805133] [INSPIRE].

[28] M. Cvetič, P. Langacker and G. Shiu, *Phenomenology of a three family standard like string model*, *Phys. Rev.* **D 66** (2002) 066004 [hep-ph/0205252] [INSPIRE].

[29] G.L. Kane, P. Kumar and J. Shao, *LHC string phenomenology*, *J. Phys.* **G 34** (2007) 1993 [hep-ph/0610038] [INSPIRE].

[30] O. Lebedev et al., *A mini-landscape of exact MSSM spectra in heterotic orbifolds*, *Phys. Lett.* **B 645** (2007) 88 [hep-th/0611095] [INSPIRE].

[31] O. Lebedev, H.P. Nilles, S. Ramos-Sanchez, M. Ratz and P.K.S. Vaudrevange, *Heterotic mini-landscape (II). Completing the search for MSSM vacua in a Z_6 orbifold*, *Phys. Lett.* **B 668** (2008) 331 [arXiv:0807.4384] [INSPIRE].

[32] H.P. Nilles, *Dynamically broken supergravity and the hierarchy problem*, *Phys. Lett.* **B 115** (1982) 193 [INSPIRE].

[33] H.P. Nilles, *Supergravity generates hierarchies*, *Nucl. Phys.* **B 217** (1983) 366 [INSPIRE].

JHEP06(2017)101

[34] S. Ferrara, L. Girardello and H.P. Nilles, *Breakdown of local supersymmetry through gauge fermion condensates*, *Phys. Lett.* **B 125** (1983) 457 [INSPIRE].

[35] H.P. Nilles, *Gaugino condensation and SUSY breakdown*, hep-th/0402022 [INSPIRE].

[36] T. Kobayashi, S. Raby and R.-J. Zhang, *Searching for realistic 4d string models with a Pati-Salam symmetry: orbifold grand unified theories from heterotic string compactification on a Z_6 orbifold*, *Nucl. Phys.* **B 704** (2005) 3 [hep-ph/0409098] [INSPIRE].

[37] H.P. Nilles, *Phenomenological hints from a class of string motivated model constructions*, *Adv. High Energy Phys.* **2015** (2015) 412487 [INSPIRE].

[38] S. Krippendorf, H.P. Nilles, M. Ratz and M.W. Winkler, *The heterotic string yields natural supersymmetry*, *Phys. Lett.* **B 712** (2012) 87 [arXiv:1201.4857] [INSPIRE].

[39] M. Badziak, S. Krippendorf, H.P. Nilles and M.W. Winkler, *The heterotic MiniLandscape and the 126 GeV Higgs boson*, *JHEP* **03** (2013) 094 [arXiv:1212.0854] [INSPIRE].

[40] L. Randall and R. Sundrum, *Out of this world supersymmetry breaking*, *Nucl. Phys.* **B 557** (1999) 79 [hep-th/9810155] [INSPIRE].

[41] G.F. Giudice, M.A. Luty, H. Murayama and R. Rattazzi, *Gaugino mass without singlets*, *JHEP* **12** (1998) 027 [hep-ph/9810442] [INSPIRE].

[42] J.A. Bagger, T. Moroi and E. Poppitz, *Anomaly mediation in supergravity theories*, *JHEP* **04** (2000) 009 [hep-th/9911029] [INSPIRE].

[43] P. Binetruy, M.K. Gaillard and B.D. Nelson, *One loop soft supersymmetry breaking terms in superstring effective theories*, *Nucl. Phys.* **B 604** (2001) 32 [hep-ph/0011081] [INSPIRE].

[44] K. Choi, A. Falkowski, H.P. Nilles, M. Olechowski and S. Pokorski, *Stability of flux compactifications and the pattern of supersymmetry breaking*, *JHEP* **11** (2004) 076 [hep-th/0411066] [INSPIRE].

[45] K. Choi, A. Falkowski, H.P. Nilles and M. Olechowski, *Soft supersymmetry breaking in KKLT flux compactification*, *Nucl. Phys.* **B 718** (2005) 113 [hep-th/0503216] [INSPIRE].

[46] J.P. Conlon, F. Quevedo and K. Suruliz, *Large-volume flux compactifications: moduli spectrum and D3/D7 soft supersymmetry breaking*, *JHEP* **08** (2005) 007 [hep-th/0505076] [INSPIRE].

[47] A. Pierce and J. Thaler, *Prospects for mirage mediation*, *JHEP* **09** (2006) 017 [hep-ph/0604192] [INSPIRE].

[48] B.L. Kaufman, B.D. Nelson and M.K. Gaillard, *Mirage models confront the LHC: Kähler-stabilized heterotic string theory*, *Phys. Rev.* **D 88** (2013) 025003 [arXiv:1303.6575] [INSPIRE].

[49] S. Kachru, R. Kallosh, A.D. Linde and S.P. Trivedi, *de Sitter vacua in string theory*, *Phys. Rev.* **D 68** (2003) 046005 [hep-th/0301240] [INSPIRE].

[50] O. Lebedev, H.P. Nilles and M. Ratz, *de Sitter vacua from matter superpotentials*, *Phys. Lett.* **B 636** (2006) 126 [hep-th/0603047] [INSPIRE].

[51] K.A. Intriligator, N. Seiberg and D. Shih, *Dynamical SUSY breaking in meta-stable vacua*, *JHEP* **04** (2006) 021 [hep-th/0602239] [INSPIRE].

[52] M. Gómez-Reino and C.A. Scrucca, *Locally stable non-supersymmetric Minkowski vacua in supergravity*, *JHEP* **05** (2006) 015 [hep-th/0602246] [INSPIRE].

JHEP06(2017)101

[53] E. Dudas, C. Papineau and S. Pokorski, *Moduli stabilization and uplifting with dynamically generated F-terms*, *JHEP* **02** (2007) 028 [hep-th/0610297] [INSPIRE].

[54] H. Abe, T. Higaki, T. Kobayashi and Y. Omura, *Moduli stabilization, F-term uplifting and soft supersymmetry breaking terms*, *Phys. Rev.* **D 75** (2007) 025019 [hep-th/0611024] [INSPIRE].

[55] O. Lebedev, V. Lowen, Y. Mambrini, H.P. Nilles and M. Ratz, *Metastable vacua in flux compactifications and their phenomenology*, *JHEP* **02** (2007) 063 [hep-ph/0612035] [INSPIRE].

[56] H. Abe, T. Higaki, T. Kobayashi and Y. Omura, *Dynamically sequestered F-term uplifting in extra dimension*, *JHEP* **04** (2008) 072 [arXiv:0801.0998] [INSPIRE].

[57] V. Lowen, H.P. Nilles and A. Zanzi, *Gaugino condensation with a doubly suppressed gravitino mass*, *Phys. Rev.* **D 78** (2008) 046002 [arXiv:0804.3913] [INSPIRE].

[58] V. Lowen and H.P. Nilles, *Mirage pattern from the heterotic string*, *Phys. Rev.* **D 77** (2008) 106007 [arXiv:0802.1137] [INSPIRE].

[59] K. Choi, K.S. Jeong and K.-i. Okumura, *Phenomenology of mixed modulus-anomaly mediation in fluxed string compactifications and brane models*, *JHEP* **09** (2005) 039 [hep-ph/0504037] [INSPIRE].

[60] A. Falkowski, O. Lebedev and Y. Mambrini, *SUSY phenomenology of KKLT flux compactifications*, *JHEP* **11** (2005) 034 [hep-ph/0507110] [INSPIRE].

[61] K. Choi, K.S. Jeong, T. Kobayashi and K.-i. Okumura, *TeV scale mirage mediation and natural little SUSY hierarchy*, *Phys. Rev.* **D 75** (2007) 095012 [hep-ph/0612258] [INSPIRE].

[62] H. Baer, V. Barger, P. Huang, A. Mustafayev and X. Tata, *Radiative natural SUSY with a 125 GeV Higgs boson*, *Phys. Rev. Lett.* **109** (2012) 161802 [arXiv:1207.3343] [INSPIRE].

[63] H. Baer et al., *Radiative natural supersymmetry: reconciling electroweak fine-tuning and the Higgs boson mass*, *Phys. Rev.* **D 87** (2013) 115028 [arXiv:1212.2655] [INSPIRE].

[64] H. Baer, V. Barger, D. Mickelson and M. Padeffke-Kirkland, *SUSY models under siege: LHC constraints and electroweak fine-tuning*, *Phys. Rev.* **D 89** (2014) 115019 [arXiv:1404.2277] [INSPIRE].

[65] H. Baer, V. Barger, H. Serce and X. Tata, *Natural generalized mirage mediation*, *Phys. Rev.* **D 94** (2016) 115017 [arXiv:1610.06205] [INSPIRE].

[66] R. Barbieri and G.F. Giudice, *Upper bounds on supersymmetric particle masses*, *Nucl. Phys.* **B 306** (1988) 63 [INSPIRE].

[67] R. Kitano and Y. Nomura, *Supersymmetry, naturalness and signatures at the LHC*, *Phys. Rev.* **D 73** (2006) 095004 [hep-ph/0602096] [INSPIRE].

[68] M. Papucci, J.T. Ruderman and A. Weiler, *Natural SUSY endures*, *JHEP* **09** (2012) 035 [arXiv:1110.6926] [INSPIRE].

[69] H. Baer, V. Barger and D. Mickelson, *How conventional measures overestimate electroweak fine-tuning in supersymmetric theory*, *Phys. Rev.* **D 88** (2013) 095013 [arXiv:1309.2984] [INSPIRE].

[70] A. Mustafayev and X. Tata, *Supersymmetry, naturalness and light higgsinos*, *Indian J. Phys.* **88** (2014) 991 [arXiv:1404.1386] [INSPIRE].

JHEP06(2017)101

[71] K.L. Chan, U. Chattopadhyay and P. Nath, *Naturalness, weak scale supersymmetry and the prospect for the observation of supersymmetry at the Tevatron and at the CERN LHC*, *Phys. Rev.* **D 58** (1998) 096004 [hep-ph/9710473] [INSPIRE].

[72] H. Baer, V. Barger and P. Huang, *Hidden SUSY at the LHC: the light higgsino-world scenario and the role of a lepton collider*, *JHEP* **11** (2011) 031 [arXiv:1107.5581] [INSPIRE].

[73] K. Choi and K.S. Jeong, *String theoretic QCD axion with stabilized saxion and the pattern of supersymmetry breaking*, *JHEP* **01** (2007) 103 [hep-th/0611279] [INSPIRE].

[74] M.R. Douglas, *The string landscape and low energy supersymmetry*, arXiv:1204.6626 [INSPIRE].

[75] J.E. Kim and H.P. Nilles, *The μ-problem and the strong CP problem*, *Phys. Lett.* **B 138** (1984) 150 [INSPIRE].

[76] K.J. Bae, H. Baer and H. Serce, *Natural little hierarchy for SUSY from radiative breaking of the Peccei-Quinn symmetry*, *Phys. Rev.* **D 91** (2015) 015003 [arXiv:1410.7500] [INSPIRE].

[77] H. Baer, V. Barger, M. Savoy and H. Serce, *The Higgs mass and natural supersymmetric spectrum from the landscape*, *Phys. Lett.* **B 758** (2016) 113 [arXiv:1602.07697] [INSPIRE].

[78] K. Choi and H.P. Nilles, *The gaugino code*, *JHEP* **04** (2007) 006 [hep-ph/0702146] [INSPIRE].

[79] D. Matalliotakis and H.P. Nilles, *Implications of nonuniversality of soft terms in supersymmetric grand unified theories*, *Nucl. Phys.* **B 435** (1995) 115 [hep-ph/9407251] [INSPIRE].

[80] P. Nath and R.L. Arnowitt, *Nonuniversal soft SUSY breaking and dark matter*, *Phys. Rev.* **D 56** (1997) 2820 [hep-ph/9701301] [INSPIRE].

[81] J.R. Ellis, K.A. Olive and Y. Santoso, *The MSSM parameter space with non-universal Higgs masses*, *Phys. Lett.* **B 539** (2002) 107 [hep-ph/0204192] [INSPIRE].

[82] J.R. Ellis, T. Falk, K.A. Olive and Y. Santoso, *Exploration of the MSSM with nonuniversal Higgs masses*, *Nucl. Phys.* **B 652** (2003) 259 [hep-ph/0210205] [INSPIRE].

[83] H. Baer, A. Mustafayev, S. Profumo, A. Belyaev and X. Tata, *Direct, indirect and collider detection of neutralino dark matter in SUSY models with non-universal Higgs masses*, *JHEP* **07** (2005) 065 [hep-ph/0504001] [INSPIRE].

[84] F.E. Paige, S.D. Protopopescu, H. Baer and X. Tata, *ISAJET 7.69: a Monte Carlo event generator for pp, $\bar{p}p$ and e^+e^- reactions*, hep-ph/0312045 [INSPIRE].

[85] H. Baer, C.-H. Chen, R.B. Munroe, F.E. Paige and X. Tata, *Multichannel search for minimal supergravity at $p\bar{p}$ and e^+e^- colliders*, *Phys. Rev.* **D 51** (1995) 1046 [hep-ph/9408265] [INSPIRE].

[86] ATLAS collaboration, *Search for squarks and gluinos in final states with jets and missing transverse momentum using 36 fb^{-1} of $\sqrt{s} = 13$ TeV pp collision data with the ATLAS detector*, ATLAS-CONF-2017-022 (2017).

[87] CMS collaboration, *Search for supersymmetry in multijet events with missing transverse momentum in proton-proton collisions at 13 TeV*, arXiv:1704.07781 [INSPIRE].

[88] H. Baer et al., *What hadron collider is required to discover or falsify natural supersymmetry?*, arXiv:1702.06588 [INSPIRE].

JHEP06(2017)101

[89] H. Baer, V. Barger and A. Mustafayev, *Implications of a 125 GeV Higgs scalar for LHC SUSY and neutralino dark matter searches*, *Phys. Rev.* **D 85** (2012) 075010 [arXiv:1112.3017] [INSPIRE].

[90] K.J. Bae, H. Baer and E.J. Chun, *Mainly axion cold dark matter from natural supersymmetry*, *Phys. Rev.* **D 89** (2014) 031701 [arXiv:1309.0519] [INSPIRE].

[91] S.P. Martin and M.T. Vaughn, *Two loop renormalization group equations for soft supersymmetry breaking couplings*, *Phys. Rev.* **D 50** (1994) 2282 [*Erratum ibid.* **D 78** (2008) 039903] [hep-ph/9311340] [INSPIRE].

[92] H. Baer, C. Balázs, P. Mercadante, X. Tata and Y. Wang, *Viable supersymmetric models with an inverted scalar mass hierarchy at the GUT scale*, *Phys. Rev.* **D 63** (2001) 015011 [hep-ph/0008061] [INSPIRE].

[93] G.F. Giudice and R. Rattazzi, *Living dangerously with low-energy supersymmetry*, *Nucl. Phys.* **B 757** (2006) 19 [hep-ph/0606105] [INSPIRE].

[94] ATLAS collaboration, *Search for a scalar partner of the top quark in the jets + $E_T^{\rm miss}$ final state at $\sqrt{s} = 13$ TeV with the ATLAS detector*, ATLAS-CONF-2017-020 (2017).

[95] CMS collaboration, *Search for top squark pair production in the single lepton final state at $\sqrt{s} = 13$ TeV*, CMS-PAS-SUS-16-051 (2017).

[96] M. Dine, A. Kagan and S. Samuel, *Naturalness in supersymmetry, or raising the supersymmetry breaking scale*, *Phys. Lett.* **B 243** (1990) 250 [INSPIRE].

[97] M.Y. Khlopov and A.D. Linde, *Is it easy to save the gravitino?*, *Phys. Lett.* **B 138** (1984) 265 [INSPIRE].

[98] K. Kohri, T. Moroi and A. Yotsuyanagi, *Big-bang nucleosynthesis with unstable gravitino and upper bound on the reheating temperature*, *Phys. Rev.* **D 73** (2006) 123511 [hep-ph/0507245] [INSPIRE].

[99] H. Baer, V. Barger, N. Nagata and M. Savoy, *Phenomenological profile of top squarks from natural supersymmetry at the LHC*, *Phys. Rev.* **D 95** (2017) 055012 [arXiv:1611.08511] [INSPIRE].

[100] ATLAS collaboration, *Prospects for benchmark supersymmetry searches at the high luminosity LHC with the ATLAS detector*, ATLAS-PHYS-PUB-2013-011 (2013).

[101] J.S. Kim, K. Rolbiecki, R. Ruiz, J. Tattersall and T. Weber, *Prospects for natural SUSY*, *Phys. Rev.* **D 94** (2016) 095013 [arXiv:1606.06738] [INSPIRE].

[102] H. Baer et al., in preparation.

[103] H. Baer et al., *Gluino reach and mass extraction at the LHC in radiatively-driven natural SUSY*, arXiv:1612.00795 [INSPIRE].

[104] H. Baer, V. Barger and M. Savoy, *Upper bounds on sparticle masses from naturalness or how to disprove weak scale supersymmetry*, *Phys. Rev.* **D 93** (2016) 035016 [arXiv:1509.02929] [INSPIRE].

[105] H. Baer et al., *Same sign diboson signature from supersymmetry models with light higgsinos at the LHC*, *Phys. Rev. Lett.* **110** (2013) 151801 [arXiv:1302.5816] [INSPIRE].

[106] H. Baer et al., *Radiatively-driven natural supersymmetry at the LHC*, *JHEP* **12** (2013) 013 [*Erratum ibid.* **06** (2015) 053] [arXiv:1310.4858] [INSPIRE].

JHEP06(2017)101

[107] C. Han et al., *Probing light higgsinos in natural SUSY from monojet signals at the LHC*, *JHEP* **02** (2014) 049 [arXiv:1310.4274] [INSPIRE].

[108] H. Baer, A. Mustafayev and X. Tata, *Monojets and mono-photons from light higgsino pair production at LHC14*, *Phys. Rev.* **D 89** (2014) 055007 [arXiv:1401.1162] [INSPIRE].

[109] P. Schwaller and J. Zurita, *Compressed electroweakino spectra at the LHC*, *JHEP* **03** (2014) 060 [arXiv:1312.7350] [INSPIRE].

[110] Z. Han, G.D. Kribs, A. Martin and A. Menon, *Hunting quasidegenerate higgsinos*, *Phys. Rev.* **D 89** (2014) 075007 [arXiv:1401.1235] [INSPIRE].

[111] H. Baer, A. Mustafayev and X. Tata, *Monojet plus soft dilepton signal from light higgsino pair production at LHC14*, *Phys. Rev.* **D 90** (2014) 115007 [arXiv:1409.7058] [INSPIRE].

[112] H. Baer, V. Barger, D. Mickelson, A. Mustafayev and X. Tata, *Physics at a higgsino factory*, *JHEP* **06** (2014) 172 [arXiv:1404.7510] [INSPIRE].

[113] H. Baer et al., *Naturalness and light higgsinos: a powerful reason to build the ILC*, PoS(ICHEP2016)156 [arXiv:1611.02846] [INSPIRE].

[114] K. Fujii et al., *The potential of the ILC for discovering new particles*, arXiv:1702.05333 [INSPIRE].

[115] K.J. Bae, H. Baer, A. Lessa and H. Serce, *Coupled Boltzmann computation of mixed axion neutralino dark matter in the SUSY DFSZ axion model*, *JCAP* **10** (2014) 082 [arXiv:1406.4138] [INSPIRE].

[116] K.J. Bae, H. Baer and E.J. Chun, *Mixed axion/neutralino dark matter in the SUSY DFSZ axion model*, *JCAP* **12** (2013) 028 [arXiv:1309.5365] [INSPIRE].

[117] H. Baer, V. Barger and H. Serce, *SUSY under siege from direct and indirect WIMP detection experiments*, *Phys. Rev.* **D 94** (2016) 115019 [arXiv:1609.06735] [INSPIRE].

[118] LUX collaboration, D.S. Akerib et al., *Results from a search for dark matter in the complete LUX exposure*, *Phys. Rev. Lett.* **118** (2017) 021303 [arXiv:1608.07648] [INSPIRE].

[119] XENON collaboration, E. Aprile et al., *Physics reach of the XENON1T dark matter experiment*, *JCAP* **04** (2016) 027 [arXiv:1512.07501] [INSPIRE].

[120] LZ collaboration, D.S. Akerib et al., *LUX-ZEPLIN (LZ) conceptual design report*, arXiv:1509.02910 [INSPIRE].

[121] FERMI-LAT and MAGIC collaborations, M.L. Ahnen et al., *Limits to dark matter annihilation cross-section from a combined analysis of MAGIC and Fermi-LAT observations of dwarf satellite galaxies*, *JCAP* **02** (2016) 039 [arXiv:1601.06590] [INSPIRE].

[122] M. Wood et al., *Prospects for indirect detection of dark matter with CTA*, in Proceedings of the *Community Summer Study 2013: Snowmass on the Mississippi (CSS2013)*, Minneapolis U.S.A. (2013) [arXiv:1305.0302] [INSPIRE].

JHEP06(2017)101